Wiley
Journal of Advanced Transportation
Volume 2025, Article ID 9971254, 26 pages
https://doi.org/10.1155/atr/9971254

WILEY

Research Article

Modeling Lane Changes at Freeway On-Ramps With a Novel Car-Following Model Based on Desired Time Headways

Moritz Berghaus [1] **and Markus Oeser** [1,2]

[1] *Institute of Highway Engineering, RWTH Aachen University, Aachen, Germany*
[2] *Federal Highway Research Institute, Bergisch Gladbach, Germany*

Correspondence should be addressed to Moritz Berghaus; berghaus@isac.rwth-aachen.de

Received 2 July 2024; Accepted 15 March 2025

Academic Editor: Mohammad Rezwan Habib

The traffic flow at freeway on-ramps is influenced not only by the lane changes made by merging vehicles but also by the longitudinal behavior of the merging vehicles and vehicles in the main lane. Existing car-following models are not suitable to represent the longitudinal behavior during merging because they are based on the idea that vehicles intend to reach a steady state, that is, constant time headway and zero speed difference, as soon as possible. At on-ramps, however, merging vehicles have time to reach this steady state until they reach the end of the on-ramp. We therefore derive a novel car-following model based on desired time headways that is able to represent this continuous adaptation toward a steady state. From this car-following model, we derive a lane change model for freeway on-ramps with seven parameters. The lane change model includes a leader selection algorithm, which enables merging vehicles to pass or be passed by vehicles in the main lane. The model also includes components to predict the lane change start time based on surrogate safety measures and to describe the lateral behavior during the lane change. Due to the resemblance to car-following models, the methodology to calibrate the lane change model at the microscopic scale can be adopted from car-following models. To validate the model, we conduct traffic simulations and compare the simulated traffic flow with trajectory data from two German freeway on-ramps. The results show that the model accurately represents the longitudinal driving behavior of merging vehicles and their followers, although it slightly overestimates the number of merging vehicles passing a vehicle in the main lane under congested traffic conditions. The simulations yield accurate headway distributions, except in cases of very risky driver behavior, and realistically capture the macroscopic speed-density relationship at the on-ramp.

1. Introduction

Microscopic traffic flow models are an important tool to assess road designs and traffic management measures, to help researchers understand traffic flow, and to study the impact of automated driving on traffic flow. They describe the longitudinal and lateral behavior of vehicles in relation to their surrounding vehicles. Microscopic traffic flow models consist of car-following models, which describe the longitudinal driving behavior, and lane change models, which describe the lateral driving behavior. Car-following models predict the acceleration of the following vehicle as a function of the gap to the leading vehicle and the speeds of the leading and following vehicle. Lane change models predict the lane change start time (lane change decision model), as well as the longitudinal and lateral acceleration during the lane change (lane change execution model), considering the positions and speeds of the surrounding vehicles in both the current lane and the target lane.

Lane changes are typically classified into desired, mandatory, and courtesy lane changes [1]. Desired lane changes, also referred to as tactical [2] or discretionary [3] lane changes, occur when a vehicle passes a slower vehicle. Mandatory (or strategic) lane changes occur when the vehicle's current lane ends or is not along its intended route, such as at on-ramps, off-ramps, or weaving sections. Courtesy (or cooperative) lane changes occur when a vehicle changes lanes to allow another vehicle to make a mandatory lane change.

Modeling the merging process at on-ramps is complex due to the different driving maneuvers in addition to the lane change itself. Merging vehicles must accelerate to reach the speed of traffic in the main lane and to reach a gap into which they can merge. This maneuver is commonly referred to as *synchronization* [4]. In dense traffic, merging vehicles accept smaller time headways during the lane change compared to regular car-following behavior, and they increase the time headway after the lane change. This maneuver is called *relaxation* [5]. In some cases, the vehicle in the main lane following the merging vehicle must facilitate the merge by making a courtesy lane change to the left or by decelerating. The former maneuver is called *anticipation* [6], the latter *cooperation* [7]. A lane change model for on-ramps must account for all these maneuvers. van Beinum et al. [8] have shown that the lane change models used in common traffic simulation packages are unable to reproduce all of these maneuvers. van Beinum et al. [8] also pointed out that the calibration of these lane change models is impractical due to the large number of parameters. The driving maneuvers at on-ramps evoke macroscopic traffic features such as the capacity drop, which means that the maximum flow in congested traffic is smaller than in free-flow traffic [9]. Chen et al. [10] have shown that congested traffic at on-ramps is also associated with riskier lane changes due to negative gaps at the start of the lane change.

Many lane change models proposed in the literature are discrete choice models focusing on criteria that must be met to perform a lane change. For example, Kesting, Treiber, and Helbing [11] proposed the MOBIL model, which includes the incentive criterion describing whether a driver intends to change lanes, and the safety criterion describing whether it is safe to change lanes. Another common approach is to model which gap a merging vehicle accepts depending on the surrounding traffic [4, 12]. The decision whether a gap is accepted or not can be described with logistic regression models that predict the probability of gap acceptance depending on the distance to the end of the on-ramp, the size of the gap, and the speed difference between the merging vehicle and its adjacent vehicles [13, 14]. The decision to start a lane change can also be modeled with game-theoretical approaches, which means that drivers intend to maximize a payoff function that depends on collision risk and speed gain [6, 15]. Laval and Leclercq [5] criticized decision-based models for being too complex and inconsistent and proposed a macroscopic lane change model in which the rate of lane changes depends on the density. Choudhury [16] argues that drivers develop a latent merging plan when they enter the on-ramp and choose their acceleration according to this plan. Other concepts to model the interaction between the merging vehicle and adjacent vehicles include lateral friction, which leads to reduced speed [17], and cooperation due to social interactions between drivers [18]. Data-driven models based on neural networks or other machine learning techniques can potentially capture merging behavior more realistically [19, 20]. While they are crucial for the development of autonomous vehicles, these black-box models do not contribute to a deeper understanding of the complexity of merging behavior.

For a complete microscopic traffic flow model that can be used in traffic simulations, lane change models must be combined with car-following models. The main challenge of these combined models is to accurately represent the longitudinal behavior during a lane change, which differs from the behavior during regular car-following [5]. Nevertheless, a regular car-following model can be applied if a vehicle in an adjacent lane can also be regarded as the leader [4, 21]. In the case of on-ramps, this assumption leads to the problem that small gaps between the merging vehicle and the leader in the main lane would result in extreme decelerations, although small gaps are not unsafe before the merging vehicle starts changing lanes. To avoid this undesired behavior, Schakel, Knoop, and van Arem [4] applied boundary conditions on the gap, which result in bounded acceleration values predicted by the car-following model. However, these boundary conditions do not ensure that the merging vehicle gradually adapts to the leader in the main lane. The model for lane changes at on-ramps proposed in this paper achieves this gradual adaptation using the idea that the merging vehicle gradually reaches a desired time headway to the leader until it reaches the end of the on-ramp.

Traffic flow models must be calibrated to find the model parameter values that minimize the deviation between real traffic and modeled traffic. The calibration of lane change models is more complex than the calibration of car-following models, which have only one output variable (acceleration) and a few input variables (speeds and positions of leader and follower). Lane change models, however, have more than one output variable (depending on the model, e.g., acceleration, lateral position, and time of the lane change) and more input variables (speeds and positions of the surrounding vehicles in the current lane and the target lane). To reduce this complexity, some studies rely on a less complex macroscopic calibration [4], while other studies observe the model parameters directly from empirical data instead of calibrating them [22]. Since our proposed model is based on a car-following model, we calibrate the model microscopically using the methodology for car-following model calibration, see [23, 24].

Traffic flow models must also be validated to show that they describe the characteristics of real traffic appropriately. The validation of lane change models can be performed at both the macroscopic and microscopic scales. Macroscopic traffic characteristics including flow, density, and mean speed describe overall traffic behavior. Criteria for validation used in the literature include the relationship between mean speed and flow [25]; speed contour plots, which visualize variations in mean speed over time and space [4]; or the distribution of flows over the lanes [4, 26, 27]. Microscopic traffic characteristics refer to the behavior of individual vehicles, for example, speed as well as gaps and headways between vehicles. In the context of on-ramps, criteria for validation include the gaps that drivers accept before they start merging [8, 13], the positions where lane changes occur, or the distribution of time headways during merging [8, 28].

The calibration of the model parameters and the validation of the models rely on empirical data. These data can

either be macroscopic flows and mean speeds, e.g., derived from induction loops, or microscopic trajectories derived from floating car data or from drones or stationary cameras. Macroscopic data from induction loops are the simplest type of data. Although they only provide cross-sectional data, these data are useful to calibrate lane change models if the cross-sections are sufficiently close together [29] or if the traffic state between the cross-sections is interpolated [30, 31], for example, using the adaptive smoothing method [32]. Floating car data provide the trajectories of a sample of vehicles, and they enable analyses on the location and duration of lane changes and the speeds during lane changes [30]. However, they do not contain interactions with other vehicles, so the gap selection and the headways during merging cannot be analyzed. Trajectory datasets from drones or stationary cameras allow detailed analyses of these aspects. Some researchers collect their own data specifically for the analysis of lane changes at on-ramps [28, 29, 33], while many others still use the NGSIM dataset from 2006 [14, 31, 34, 35]. For all data sources, it is important that both free and congested traffic states are included to achieve a model that is valid for both states.

In this paper, we derive a lane change model for freeway on-ramps based on a car-following model that uses the concept of desired time headways (Section 2). Since the lane change model is derived from a car-following model, the methodology for calibrating and validating the model at the microscopic scale can be adopted from car-following models (Section 3). We analyze the features of the model using sensitivity analysis, example cases, and traffic simulations (Section 4).

2. Model Derivation

We propose a model for lane changes at on-ramps that focuses on the longitudinal behavior, which means it is based on a car-following model with the following adaptations:

1. The merging vehicle (hereafter referred to as *merger*) may have more than one leader (see Figure 1(a): one on the on-ramp and one in the main lane). The car-following model calculates one acceleration value for each leader. The smaller value is the relevant one. In the following, we use the term *leader* for the leader in the main lane if not mentioned otherwise because this is the relevant leader in most cases.
2. While the merger is on the on-ramp, it can pass one or more vehicles in the main lane or be passed by them (see Figure 1(b)). Thus, the leader is not necessarily the current preceding vehicle, but the preceding vehicle after merging. The algorithm for selecting the leader will be presented in Section 2.5.
3. The merger must reach a sufficient time headway (hereafter referred to as *headway*) to the leader only at the end of the on-ramp, while smaller and even negative headways are allowed at the beginning of the on-ramp, as shown in Figure 1(b). When the lane change starts, the headway must be at least zero, i.e., the merger must be behind the leader.
4. The follower in the main lane also has more than one leader: one in the main lane, which is also the leader of the merger, and the merger. The headway between the follower and the merger must also only be sufficient at the end of the on-ramp, and it must be at least zero when the lane change starts. Again, the car-following model calculates one acceleration value for each leader, and the smaller value is the relevant one.

While adaptation 1 can easily be achieved with any existing car-following model, adaptations 2, 3, and 4 are incompatible with existing car-following models because the models would predict unrealistically negative accelerations if the headway was small or negative. Therefore, we propose a new car-following model based on desired headways, which we describe in the following section. From this car-following model, we derive the lane change model for on-ramps.

2.1. Car-Following Model Based on Desired Time Headways. The proposed car-following model is based on the concept that the follower intends to achieve a desired headway T_{des} to the leader. The headway T at time t is defined as the net distance between leader and follower divided by the speed of the follower:

$$T(t) = \frac{\Delta x(t)}{v_F(t)} = \frac{x_L(t) - x_F(t) - (L_L/2) - (L_F/2) - \Delta x_{\min}}{v_F(t)}, \tag{1}$$

where x is the position, v is the speed, and L is the length of a vehicle. Δx represents the net distance between leader and follower minus a minimum distance $\Delta x_{\min}$ at standstill. $\Delta x_{\min}$ is included here to make the model equations more comprehensible, although it is not included in the common definition of the net distance. Index L denotes the leader, and index F denotes the follower.

The follower accelerates with acceleration a_F such that it reaches the desired headway after time τ, which we refer to as *adaptation time*. To derive this acceleration, we use the following kinematic equations, assuming the leader has zero acceleration, which is a common simplification in existing car-following models, e.g., in the intelligent driver model (IDM) [36]:

$$x_F(t+\tau) = \frac{1}{2} \cdot a_F(t) \cdot \tau^2 + v_F(t) \cdot \tau + x_F(t), \tag{2}$$

$$v_F(t+\tau) = a_F(t) \cdot \tau + v_F(t), \tag{3}$$

$$x_L(t+\tau) = v_L(t) \cdot \tau + x_L(t). \tag{4}$$

After the adaptation time, the headway must be equal to the desired headway:

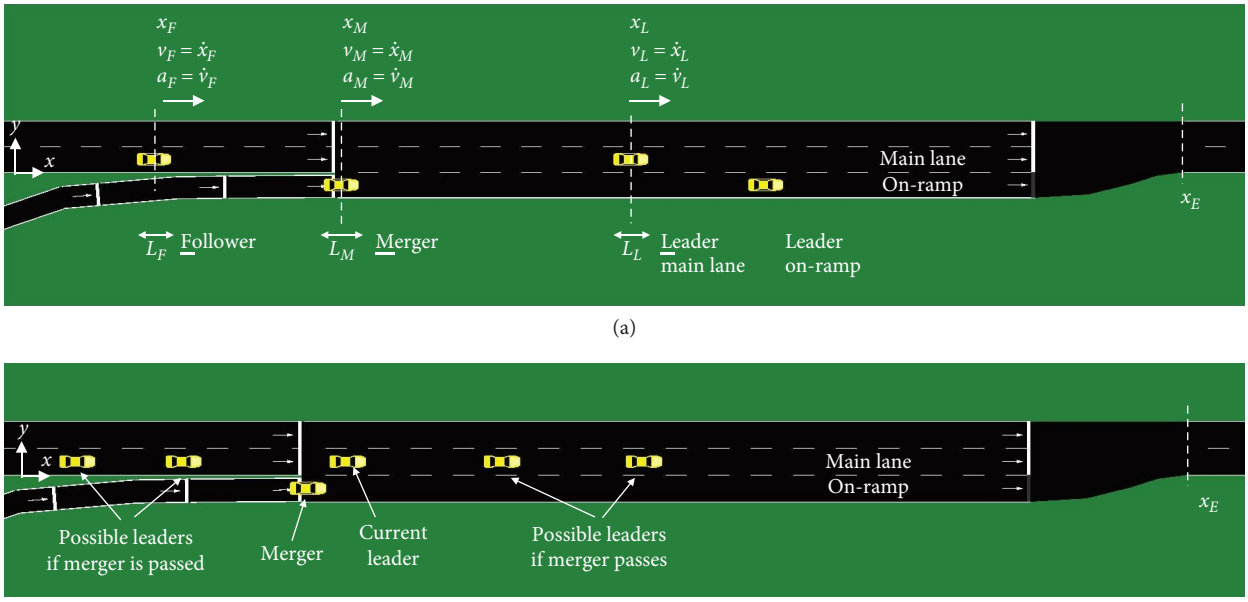

FIGURE 1: (a) Definition of leader, follower, and merger, (b) small headway between merger and current leader at the beginning of the on-ramp, and possible leaders if merger passes or is passed.

$$T(t+\tau) = \frac{\Delta x(t+\tau)}{v_F(t+\tau)} = \frac{x_L(t+\tau) - x_F(t+\tau) - (L_L/2) - (L_F/2) - \Delta x_{\min}}{v_F(t+\tau)} = T_{\text{des}}. \tag{5}$$

Inserting equations (2)–(4) into equation (5) yields:

$$\frac{v_L \cdot \tau + x_L(t) - (1/2)a_F(t) \cdot \tau^2 - v_F(t) \cdot \tau - x_F(t) - (L_L/2) - (L_F/2) - \Delta x_{\min}}{a_F(t) \cdot \tau + v_F(t)} = T_{\text{des}}. \tag{6}$$

Equation (6) can be solved for a_F:

$$a_F(t) = \frac{v_L(t) \cdot \tau + x_L(t) - v_F(t) \cdot (\tau + T_{\text{des}}) - x_F(t) - (L_L/2) - (L_F/2) - \Delta x_{\min}}{(1/2)\tau^2 + \tau \cdot T_{\text{des}}} = \frac{v_L(t) \cdot \tau - v_F(t) \cdot (\tau + T_{\text{des}}) + \Delta x(t)}{(1/2)\tau^2 + \tau \cdot T_{\text{des}}}. \tag{7}$$

The result of equation (7) is dominated by τ^2 in the denominator, which means smaller values of τ lead to larger absolute values of the acceleration. The adaptation time τ can thus be interpreted as the urgency with which the follower intends to reach the desired headway, where smaller values of τ represent a higher urgency. This urgency should depend on the current headway $T(t)$. If the current headway is small, the follower must urgently reach the desired headway to avoid a collision. If the current headway is large, the follower has sufficient time to reach the desired headway. For simplicity, we assume that τ is equal to the current headway. However, τ must have an upper bound because otherwise the absolute value of the acceleration would be very small if the headway is very large, which occurs for small speeds ($v_F \longrightarrow 0$) or large distances ($\Delta x \longrightarrow \infty$):

$$\tau(t) = \min(T(t), \tau_{\max}), \tag{8}$$

where the upper bound $\tau_{\max}$ can be interpreted as the headway above which the leader does not influence the behavior of the follower. Since this parameter is only relevant in a few situations, it does not have to be calibrated. We select $\tau_{\max} = 10\,\text{s}$.

To avoid physically impossible accelerations, a_F should be bounded by a minimum (negative) acceleration $a_{\min}$ and a maximum (positive) acceleration $a_{\max}$. The acceleration is additionally bounded by $-v_F(t)/\tau$ to avoid negative speeds

after the adaptation time and by $v_{\max} - v_F(t)/\tau$ to avoid speeds above the maximum desired speed $v_{\max}$. As a result, the model equation of the car-following model based on desired time headways is as follows:

$$a_{F,\mathrm{DTH}}(t) = \max\left[\min\left(\frac{v_L(t)\cdot\tau - v_F(t)\cdot\left(\tau + T_{\mathrm{des}}\right) + \Delta x(t)}{(1/2)\tau^2 + \tau\cdot T_{\mathrm{des}}}, a_{\max}, \frac{v_{\max} - v_F(t)}{\tau}\right), a_{\min}, -\frac{v_F(t)}{\tau}\right]. \tag{9}$$

In summary, the car-following model has five parameters listed in Table 1.

These parameters have an intuitive physical meaning and can either be calibrated or directly observed or estimated from real traffic data. They are also similar to the parameters of other common car-following models, for example, the IDM with v_0, a, b, s_0, and T [36]. While the IDM uses v_0, a, and b in all driving situations, our model uses these parameters only to bound the acceleration (see equation (9)).

2.2. Car-Following Model for Mergers at On-Ramps. To model the acceleration of the merger in the case of on-ramps, the car-following model presented in Section 2.1 is adapted. For now, we assume that the merger has already selected a leader behind which it will merge. The selection of the leader will be modeled in Section 2.5. The merger aims at reaching the desired headway until it reaches the end of the on-ramp, and it also aims at reaching a non-negative headway before it starts the lane change.

First, we describe the former situation (desired headway until the end of the on-ramp), which is shown in Figure 2. The proposed car-following model can be applied in this situation by changing the definition of the adaptation time τ in equation (6). In the case of on-ramps, the adaptation time is the time until the merger reaches the end of the on-ramp, which we denote as τ_E. Thus, small headways or large speed differences between merger and leader at the beginning of the on-ramp do not result in extreme negative accelerations because there is enough time for the merger to reach the desired headway.

To derive the acceleration $a_{M,\mathrm{DesiredHeadway}}$ of the merger, we use the same kinematic equations (2)–(4) as above, but using index M instead of F. The position of the merger after the adaptation time τ_E is equal to the position of the end of the on-ramp x_E. Since the time until the end of the on-ramp depends on the acceleration, equation (2) is first solved for a_M:

$$a_{M,\mathrm{DesiredHeadway}}(t) = \frac{2\left(x_E - v_M(t)\cdot\tau_E - x_M(t)\right)}{\tau_E^2}. \tag{10}$$

Equation (10) is then inserted for a_M into equation (6):

$$\begin{aligned}
&\frac{v_L(t)\cdot\tau_E + x_L(t) - (1/2)a_{M,\mathrm{DesiredHeadway}}(t)\cdot\tau_E^2 - v_M(t)\cdot\tau_E - x_M(t) - \left(L_L/2\right) - \left(L_M/2\right) - \Delta x_{\min}}{a_{M,\mathrm{DesiredHeadway}}(t)\cdot\tau_E + v_M(t)} \\
&= \frac{v_L(t)\cdot\tau_E + x_L(t) - \left(x_E - v_M(t)\cdot\tau_E - x_M(t)\right) - v_M(t)\cdot\tau_E - x_M(t) - \left(L_L/2\right) - \left(L_M/2\right) - \Delta x_{\min}}{2\left(\left(x_E - v_M(t)\cdot\tau_E - x_M(t)\right)/\tau_E\right) + v_M(t)} = T_{\mathrm{des}} \\
&\iff v_L(t)\cdot\tau_E^2 + \left(x_L(t) - x_E - \frac{L_L}{2} - \frac{L_M}{2} - \Delta x_{\min} + T_{\mathrm{des}}\cdot v_M(t)\right)\cdot\tau_E - 2\cdot T_{\mathrm{des}}\cdot\left(x_E - x_M(t)\right) = 0.
\end{aligned} \tag{11}$$

This quadratic equation is solved for τ_E:

$$\tau_E = \frac{-x_L(t) + x_E + \left(L_L/2\right) + \left(L_M/2\right) + \Delta x_{\min} - T_{\mathrm{des}}\cdot v_M(t) \pm \sqrt{\left(x_L(t) - x_E - \left(L_L/2\right) - \left(L_M/2\right) - \Delta x_{\min} + T_{\mathrm{des}}\cdot v_M(t)\right)^2 + 8\cdot v_L(t)\cdot T_{\mathrm{des}}\cdot\left(x_E - x_M(t)\right)}}{2\cdot v_L(t)}. \tag{12}$$

Only real and positive solutions of equation (12) are valid because the end of the on-ramp is reached in the future. If equation (12) has two real and positive solutions, the smaller one is relevant because it corresponds to the nearest moment in the future. This solution is then inserted into equation (10) to obtain the acceleration of the merger. If equation (12) has no real and positive solution, the resulting acceleration of the merger would be so small that it stops before the end of the

Table 1: Parameters of the car-following model based on desired headways.

$v_{\max}$	Maximum desired speed	m/s
$a_{\max}$	Maximum (positive) acceleration	m/s^2
$a_{\min}$	Minimum (negative) acceleration	m/s^2
$\Delta x_{\min}$	Minimum distance at standstill	m
T_{des}	Desired headway	s

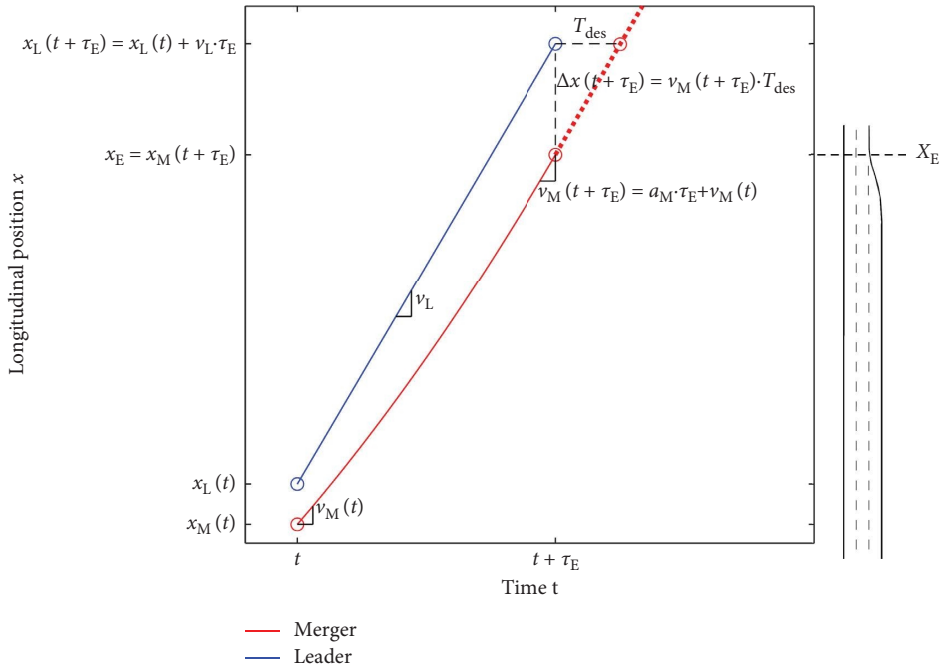

Figure 2: Time–space diagram with a merger (M) and its leader (L). The merger accelerates with a_M such that the net headway is equal to the desired headway T_{des} when it reaches the end of the on-ramp x_E after time τ_E. Note that the time–space diagram shows the gross distance and headway instead of the net distance and headway because it does not show the lengths of the vehicles.

on-ramp. In this case, it can be assumed that the merger stops at the end of the on-ramp. Equation (3) thus becomes:

$$\begin{aligned} & v_M(t+\tau_E) = a_M(t) \cdot \tau_E + v_M(t) = 0 \\ & \Longleftrightarrow \frac{2(x_E - v_M(t) \cdot \tau_E - x_M(t))}{\tau_E^2} \cdot \tau_E + v_M(t) = 0 \\ & \Longleftrightarrow \tau_E = \frac{2(x_E - x_M(t))}{v_M(t)}. \end{aligned} \tag{13}$$

For the latter situation (non-negative headway when the lane change starts), which is shown in Figure 3, the proposed car-following model can also be applied by changing the desired headway to zero ($T_{\text{des}} = 0$) and the time until the desired headway is reached to the time until the lane change starts. To finish the lane change at the end of the on-ramp at $t + \tau_E$, the lane change must start at $t + \tau_E - \tau_{\text{LC}}$, where τ_{LC} is the duration of the lane change. τ_{LC} is another parameter of the proposed lane change model for on-ramps in addition to the parameters of the car-following model introduced in Section 2.1. The time until the lane change starts is denoted as $\tau_{\text{ZeroHeadway}} = \tau_E - \tau_{\text{LC}}$. Inserting $T_{\text{des}} = 0$ and $\tau_{\text{ZeroHeadway}}$ instead of τ into equation (7) and adapting the indices, the acceleration of the merger is obtained:

$$a_{M,\text{ZeroHeadway}(t)} = \frac{(v_L(t) - v_M(t)) \cdot \tau_{\text{ZeroHeadway}} + \Delta x(t)}{(1/2)\tau_{\text{ZeroHeadway}}^2}. \tag{14}$$

After the lane change has started, the merger also wants to maintain a non-negative headway. In this case, $\tau_{\text{ZeroHeadway}}$ can be set equal to the current headway.

The resulting acceleration of the merger is the minimum of the two accelerations mentioned above to ensure that the headway at the end of the on-ramp is at least the desired headway and that the headway at the start of the lane change is non-negative. Additionally, the bounds introduced in equation (9) are applied:

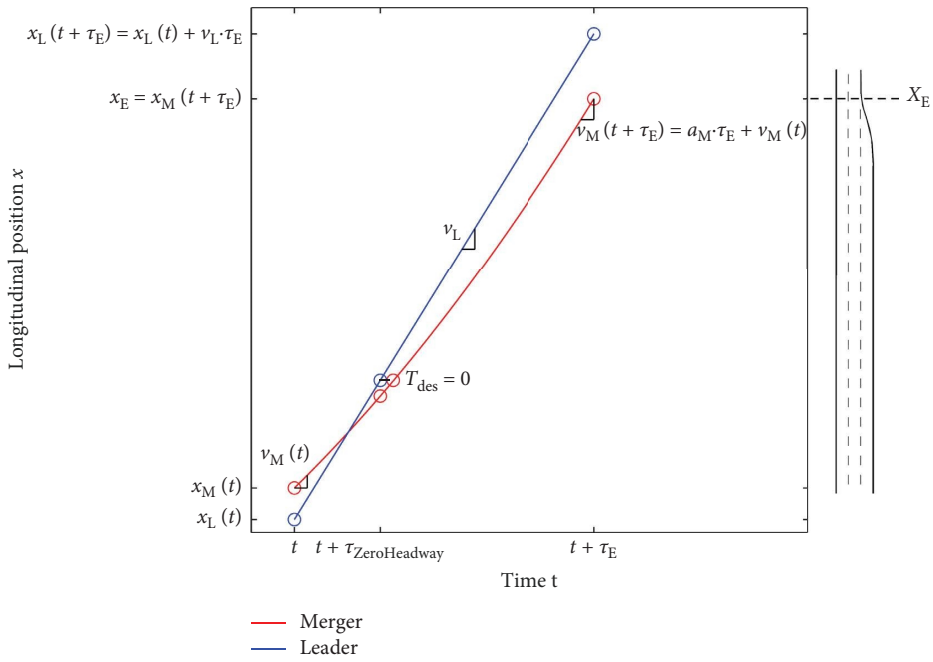

FIGURE 3: Time–space diagram with a merger (M) and its leader (L). The merger accelerates with a_M such that the net headway is zero when it starts the lane change after time $\tau_{ZeroHeadway}$. Note that the time–space diagram shows the gross headway, which is larger than zero, instead of the net headway because it does not show the lengths of the vehicles.

$$a_M(t) = \max\left(\min\left(a_{M,DesiredHeadway}(t), a_{M,ZeroHeadway}(t), a_{max}, \frac{v_{max} - v_F(t)}{\tau_{ZeroHeadway}}\right), a_{min}, -\frac{v_F(t)}{\tau_{ZeroHeadway}}\right). \tag{15}$$

2.3. Lane Change Start. So far, we have focused on the longitudinal behavior of the merger. To model the lateral behavior, the most essential factor is the time when the lane change starts. In Section 2.2, we have assumed that the lane change starts at the latest possible time, that is, such that the lane change is completed when the merger reaches the end of the on-ramp. However, it is intuitive to assume that mergers start the lane change earlier if it is safe.

To quantify the level of safety, surrogate safety measures (SSMs) are suitable. For example, the *Deceleration Rate to Avoid a Crash* (DRAC) describes the required acceleration of the follower to reach a zero headway assuming that the leader does not change its speed, see [37]:

$$\text{DRAC} = \begin{cases} -\infty, & \text{if } x_L - x_F - \frac{L_L}{2} - \frac{L_F}{2} \le 0, \\ 0, & \text{if } x_L - x_F - \frac{L_L}{2} - \frac{L_F}{2} > 0 \text{ and } v_L \ge v_F, \\ -\frac{(v_L - v_F)^2}{2(x_L - x_F - (L_L/2) - (L_F/2))}, & \text{if } x_L - x_F - \frac{L_L}{2} - \frac{L_F}{2} > 0 \text{ and } v_L < v_F. \end{cases} \tag{16}$$

If both the DRAC between the merger (index M instead of F in equation (16)) and the leader and between the follower and the merger (index M instead of L in equation (16)) are larger than some threshold DRAC_{min}, the lane change can start safely. In this case, the adaptation time τ becomes the time until the lane change is completed and not the time the merger reaches the end of the on-ramp.

Even if $\text{DRAC} \ge \text{DRAC}_{min}$ is not fulfilled until the latest possible lane change start time, the lane change can safely start because the car-following model for mergers (see Section 2.2) ensures that the headway between leader and merger is non-negative at this moment. To ensure that the headway between merger and follower is also non-negative, the follower must cooperate by decelerating in some cases. This cooperation will be described in Section 2.6.

In summary, the lane change model has the same five parameters as the car-following model (see Table 1) and two additional parameters (see Table 2). Compared to lane change models from the literature [4, 11, 12], the number of parameters in our model is small, which facilitates the calibration and the interpretability of the model parameters.

2.4. Lateral Position During the Lane Change. After the lane change has started, the merger changes its lateral position from the center of the on-ramp to the center of the main lane. The lateral position during the lane change $y_M(t)$ follows some s-shaped curve (see Figure 4). Given that t_0 is the time when the lane change starts, $y = 0$ is the edge between the on-ramp and the main lane, and W_{Lane} is the lane width, the following boundary conditions for the lateral position and its first derivative $\dot{y}_M(t)$ apply:

$$y_M(t_0) = -\frac{W_{\text{Lane}}}{2}, \tag{17}$$

$$\dot{y}_M(t_0) = 0, \tag{18}$$

$$y_M(t_0 + \tau_{\text{LC}}) = \frac{W_{\text{Lane}}}{2}, \tag{19}$$

$$\dot{y}_M(t_0 + \tau_{\text{LC}}) = 0. \tag{20}$$

These boundary conditions ensure that the merger is in the center of the lane before and after the lane change (equations (17) and (19)) and that the merger has no lateral movement before and after the lane change (equations (18) and (20)).

The simplest solution for an s-shaped curve fulfilling these boundary conditions is the following third-order polynomial:

$$y_M(t) = \begin{cases} -\dfrac{W_{\text{Lane}}}{2}, & t < t_0, \\ \dfrac{-2W_{\text{Lane}}}{\tau_{\text{LC}}^3}(t - t_0)^3 + \dfrac{3W_{\text{Lane}}}{\tau_{\text{LC}}^2}(t - t_0)^2 - \dfrac{W_{\text{Lane}}}{2}, & t_0 \le t \le t_0 + \tau_{\text{LC}}, \\ \dfrac{W_{\text{Lane}}}{2}, & t > t_0 + \tau_{\text{LC}}, \end{cases} \tag{21}$$

$$\dot{y}_M(t) = \begin{cases} 0, & t < t_0 \vee t > t + \tau_{\text{LC}}, \\ \dfrac{-6W_{\text{Lane}}}{\tau_{\text{LC}}^3}(t - t_0)^2 + \dfrac{6W_{\text{Lane}}}{\tau_{\text{LC}}^2}(t - t_0), & t_0 \le t \le t_0 + \tau_{\text{LC}}. \end{cases} \tag{22}$$

2.5. Selection of the Leader. When a merger enters the on-ramp, there is usually more than one vehicle nearby in the main lane, which could be potential leaders of the merger. The merger selects a gap, which means it decides for one of these vehicles as a leader. This decision depends on its distances to the vehicles in the main lane, the gaps between them and their speeds. Although a human driver makes this decision intuitively, we aim to represent this decision in the lane change model using the concept of desired headways. To this end, we assume that the merger intends to reach the desired headway not only to the leader, but also to the follower. Accordingly, it must consider the follower even though this contradicts the concept of a car-following model, where only the leader determines the driving behavior. We argue that this modification is required to select the appropriate leader. The required acceleration to reach the desired headway to the leader has been derived in Section 2.2, while the required acceleration to reach the desired headway to the follower will be derived now.

When the merger reaches the end of the on-ramp x_E, the headway to the follower equals the desired headway T_{des}:

$$T_{\text{des}} = \frac{x_E - x_F\left(t + \tau_{E,\text{Fol.}}\right) - \left(L_M/2\right) - \left(L_F/2\right) - \Delta x_{\min}}{v_F\left(t + \tau_{E,\text{Fol.}}\right)}, \tag{23}$$

where $\tau_{E,\text{Fol.}}$ is the time until the merger reaches the end of the on-ramp, assuming that it accelerates such that it reaches the desired headway to the follower after $\tau_{E,\text{Fol.}}$. For simplicity, we assume that the follower in the main lane maintains its speed, which means that $v_F(t + \tau_{E,\text{Fol.}}) = v_F(t)$ and $x_F(t + \tau_{E,\text{Fol.}}) = v_F(t) \cdot \tau_{E,\text{Fol.}} + x_F(t)$. With this simplification, equation (23) can be solved for $\tau_{E,\text{Fol.}}$:

$$\tau_{E,\text{Fol.}} = \frac{x_E - x_F(t) - \left(L_M/2\right) - \left(L_F/2\right) - \Delta x_{\min}}{v_F(t)} - T_{\text{des}}. \tag{24}$$

This solution can be inserted into equation (10) to obtain the acceleration of the merger that is required to reach the desired headway to the follower in the main lane:

$$a_{M,\text{Fol.}}(t) = \frac{2\left(x_E - v_M(t) \cdot \tau_{E,\text{Fol.}} - x_M(t)\right)}{\tau_{E,\text{Fol.}}^2}. \tag{25}$$

Table 2: Additional parameters of the lane change model.

τ_{LC}	Lane change duration	s
$\mathrm{DRAC}_{\mathrm{min}}$	Threshold for lane change start	$\mathrm{m/s^2}$

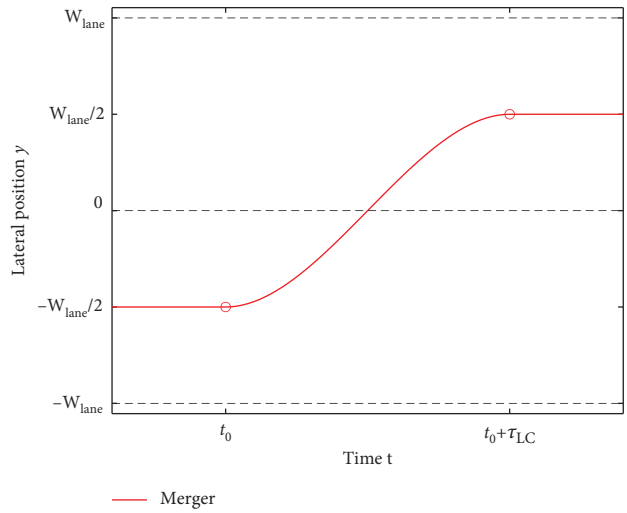

Figure 4: Lateral position of the merger. The lane change starts at t_0 and ends at $t_0 + \tau_{LC}$. Before and after the lane change, the merger drives in the center of the lane, and during the lane change, it follows an s-shaped curve.

Note that $a_{M,\mathrm{Fol.}}$ is a lower bound because larger accelerations lead to headways between merger and follower that are larger than the desired headway. a_M, on the other hand, is an upper bound because smaller accelerations lead to headways between leader and merger that are larger than the desired headway.

To select a leader, the merger evaluates $a_{M,i}$ and $a_{M,\mathrm{Fol.},i}$ for every hypothetical leader i and the corresponding follower. The smallest values of a_M and $a_{M,\mathrm{Fol.}}$ are obtained for vehicles far behind the merger, and the largest values are obtained for vehicles far in front of the merger. The larger the difference between a_M and $a_{M,\mathrm{Fol.}}$ for a given leader and follower, the larger the gap between leader and follower is. Therefore, the merger wants to select a gap for which the difference between a_M and $a_{M,\mathrm{Fol.}}$ is large.

To reach the gap between a hypothetical leader and follower that is not the current leader and follower, the merger must pass a vehicle in the main lane or be passed by a vehicle in the main lane. Passing or being passed is only possible if it is completed before the merger must start its lane change. Completed means that the merger has a nonnegative net distance to the hypothetical leader and follower. This condition can be represented by the following equations:

$$x_M\left(t+\tau_{\mathrm{Pass},i}\right)-x_i\left(t+\tau_{\mathrm{Pass},i}\right)-\frac{L_M}{2}-\frac{L_i}{2}-\Delta x_{\min}\geq 0,\quad \forall i \mid x_i(t)>x_M(t), \tag{26}$$

$$x_i\left(t+\tau_{\mathrm{Pass},i}\right)-x_M\left(t+\tau_{\mathrm{Pass},i}\right)-\frac{L_i}{2}-\frac{L_M}{2}-\Delta x_{\min}\geq 0,\quad \forall i \mid x_i(t)\leq x_M(t), \tag{27}$$

where $\tau_{\mathrm{Pass},i}$ denotes the available time for the merger to pass vehicle i or being passed by vehicle i:

$$\tau_{\mathrm{Pass},i}=\begin{cases}\tau_{E,i+1}-\tau_{\mathrm{LC}}, & x_i(t)>x_M(t),\\ \tau_{E,i}-\tau_{\mathrm{LC}}, & x_i(t)\leq x_M(t).\end{cases} \tag{28}$$

The difference between the two cases in equation (28) is that the merger has vehicle $i+1$ (the leader of vehicle i) as a leader if it passes vehicle i, whereas the merger has vehicle i as the leader if it is passed by vehicle i.

The positions at time $t+\tau_{\mathrm{Pass},i}$ can be computed assuming that the vehicles in the main lane maintain their speed (using equation (3) adjusting the indices) and that the merger accelerates with $a_{M,i}$ or $a_{M,i+1}$, depending on the case in equation (28), using equation (2) adjusting the indices. Only vehicles that can pass the merger or that can be passed by the merger before the lane change must start (equation (26) or (27)) are considered as potential leaders. Of these potential leaders, the merger selects the one for which the corresponding leader and follower yield the largest difference between a_M and $a_{M,\mathrm{Fol.}}$, i.e., it selects the largest reachable gap. If this difference is negative, the acceleration to reach the desired headway to the leader is smaller than the acceleration to reach the desired headway to the follower. In this case, the merger must rely on the cooperation of the follower, i.e., the follower must decelerate to enable the desired headway. The behavior of the follower in this case will be described in Section 2.6.

2.6. Car-Following Model for the Follower Behind a Merger. After the merger M has merged into the gap between leader L and follower F, M becomes the new leader of vehicle F. During the preparation and execution of the lane change, however, vehicle F has two leaders (L and M). The interaction between F and L is a normal car-following situation, so it can be described by the car-following model introduced in Section 2.1. For the interaction between F and

M, the same concept as for the interaction between M and L can be applied. That means vehicle F intends to reach the desired headway to M until M has completed its lane change. Additionally, F intends to reach a non-negative headway until the latest possible time the merger starts its lane change. We assume that the drivers of vehicles in the main lane can perceive which gap M has selected for merging even before the lane change has started by estimating the acceleration of M. As a result, only the vehicle behind the gap that M merges into considers M as a leader and is defined as F. In conformity with the idea of car-following models, we assume that vehicle M only influences vehicle F if M is in front of F. That means if M passes F, it will influence F only after the passing maneuver is completed. The acceleration of F to reach the desired headway can be modeled by adapting equation (1). However, the simplification made in Section 2.2 that the leader (in this case vehicle M) has zero acceleration is not valid because the acceleration of the merger significantly influences the future headway. Equation (6) therefore becomes:

$$\frac{(1/2)a_M(t)\cdot\tau^2 + v_M\cdot\tau + x_M(t) - (1/2)a_F(t)\cdot\tau^2 - v_F(t)\cdot\tau - x_F(t) - \left(L_M/2\right) - \left(L_F/2\right) - \Delta x_{\min}}{a_F(t)\cdot\tau + v_F(t)} = T_{\text{des}}. \tag{29}$$

To compute the acceleration to reach the desired headway after the lane change, $\tau = \tau_E$ is used. Solving equation (29) for a_F yields:

$$a_{F,\text{DesiredHeadway}}(t) = \frac{(1/2)a_M(t)\cdot\tau_E^2 + v_M(t)\cdot\tau_E + x_M(t) - v_F(t)\cdot\left(\tau_E + T_{\text{des}}\right) - x_F(t) - \left(L_M/2\right) - \left(L_F/2\right) - \Delta x_{\min}}{(1/2)\tau_E^2 + \tau_E\cdot T_{\text{des}}}. \tag{30}$$

To compute the acceleration to reach a non-negative headway when the lane change starts, $\tau_{\text{ZeroHeadway}} = \tau_E - \tau_{LC}$ and $T_{\text{des}} = 0$ are used. In this case, equation (29) yields:

$$a_{F,\text{ZeroHeadway}}(t) = \frac{(1/2)a_M(t)\cdot\tau_{\text{ZeroHeadway}}^2 + \left(v_M(t) - v_F(t)\right)\cdot\tau_{\text{ZeroHeadway}} + x_M(t) - x_F(t) - \left(L_M/2\right) - \left(L_F/2\right) - \Delta x_{\min}}{(1/2)\tau_{\text{ZeroHeadway}}^2}. \tag{31}$$

The resulting equation for the acceleration of the follower including the appropriate bounds is:

$$a_F(t) = \max\left(\min\left(a_{F,\text{DesiredHeadway}}(t), a_{F,\text{ZeroHeadway}}(t), a_{\max}, \frac{v_{\max} - v_F(t)}{\tau_{\text{ZeroHeadway}}}\right), a_{\min}, -\frac{v_F(t)}{\tau_{\text{ZeroHeadway}}}\right). \tag{32}$$

3. Model Calibration and Validation

In this section, we describe the trajectory data used for calibration and validation as well as the methodology to calibrate and validate the proposed lane change model.

3.1. Trajectory Data. We use trajectory data from two different on-ramp locations with different infrastructure designs and traffic conditions. The main differences between the two locations are the number of lanes, the speed limit, and the length of the on-ramp (see Table 3). The first dataset was collected by our research group, including the authors of this paper, following the methodology described in [38] with some adaptations in the computer vision algorithms. The trajectories contain an on-ramp on the freeway A59 in Duisburg, Germany (see Figure 5). The trajectories have been gathered from drone videos recorded during the morning peak (06:30 to 07:15) in August 2022. The second dataset is part of the exiD dataset by Moers et al. [39]. The trajectories contain an on-ramp on the freeway A4 in Cologne, Germany. The data were recorded during the afternoon peak (approximately 14:00 to 17:00) in 2021. While the Duisburg dataset contains almost only congested traffic, the Cologne dataset contains mostly free-flow traffic

Table 3: Overview of the two trajectory datasets.

	Duisburg dataset	Cologne dataset
Location	A59, Duisburg Meiderich, Germany	A4, Cologne Klettenberg, Germany
Number of lanes	2 + on-ramp	3 + on-ramp
Length of the on-ramp	ca. 100 m	ca. 200 m
Length of the road section	ca. 540 m	ca. 400 m
Speed limit	80 km/h	120 km/h
Total duration	38 min	102 min
Number of trajectories	2834 (≈4475 vehicles per hour)	7039 (≈4141 vehicles per hour)
Number of mergers	262 (≈414 vehicles per hour)	581 (≈342 vehicles per hour)

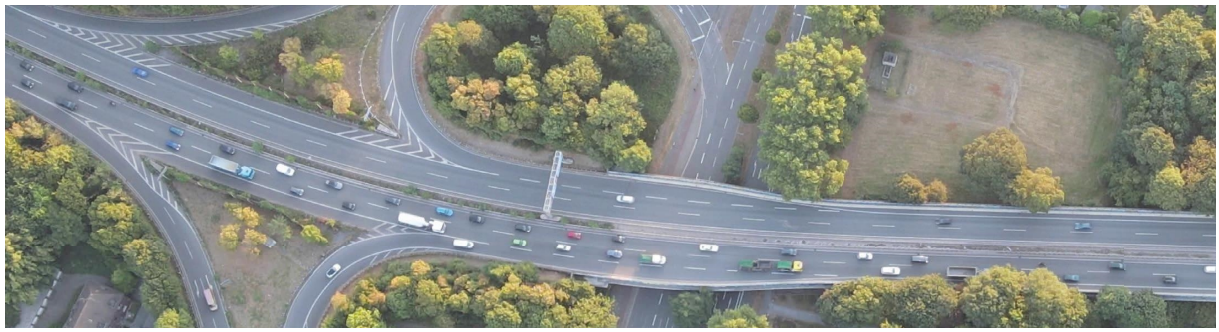

Figure 5: Screenshot of the drone video of freeway A59 in Duisburg, Germany. The on-ramp is at the bottom of the image (travel direction left to right).

with a short period of congested traffic. Both datasets are split into two equally long parts, one for calibration and one for validation.

3.2. Calibration Methodology. The aim of the model calibration is to obtain those values of the model parameters for which the prediction error is minimal. To achieve a model that accurately represents the driver behavior at the microscopic scale, we calibrate the model microscopically. Since our lane change model is based on the concept of a car-following model, we can adopt the methodology of car-following model calibration, which has been extensively discussed in the literature, see [23, 24]. Consequently, we define the prediction error as the deviation between the observed trajectories and the trajectories predicted by the model. We assume that the behavior of all drivers can be represented by the same model parameter values, i.e., we assume that the model is deterministic, which simplifies the calibration process.

We divide the calibration process into three different cases according to the three submodels described in Section 2: (1) mergers, (2) followers of mergers, and (3) vehicles with normal car-following behavior, i.e., all vehicles except the mergers and their followers. Although these submodels share the same model parameters, the values of these parameters may be different due to the different driving behaviors in each of these situations.

The model for mergers (submodel 1, Sections 2.2–2.5) consists of four different components (car-following, lane change start, lateral position, and leader selection). Since all model parameters affect more than one of these components, we calibrate the model in its entirety without separating it into its components. By minimizing the deviation between the observed and modeled trajectories, the best model parameter values for all components are obtained. For example, selecting the correct leader reduces the deviation in longitudinal direction, and predicting the correct lane change start time reduces the deviation in lateral direction.

Mergers whose leader or follower make a courtesy lane change are excluded from the calibration process. Mergers that change into the left lane directly after merging are also excluded.

To obtain the modeled trajectories, we select the time when a merger is at the start of the on-ramp as initial condition. We assume that the speed and position of the merger and the current positions and speeds of all vehicles in the main lane are known. Based on this information, the model decides which leader is selected and whether the lane change is started or not and predicts the acceleration and the lateral position. The acceleration is used to compute the speed and position at the next time step. We assume that a time step of 0.1 s is a good balance between computational efficiency and accuracy. At the next time step, this process is repeated with the predicted speed and position of the merger and the observed speeds and positions of the vehicles in the main lane. Thus, we neglect that the behavior of the mergers might influence the vehicles in the main lane to simplify the calibration. This process is repeated until the time when the merger reaches the end of the on-ramp. For each time step, the deviation between the predicted and the observed position is computed. This method is referred to as global calibration [23]. With the deviations, the root mean square error (RMSE) of the trajectory is computed:

$$\mathrm{RMSE}_{\mathrm{Trajectory}} = \sqrt{\frac{1}{n}\left(\sum_{i=1}^{n}\left(x_{\mathrm{Mod.}} - x_{\mathrm{Obs.}}\right)^2 + \sum_{i=1}^{n}\left(y_{\mathrm{Mod.}} - y_{\mathrm{Obs.}}\right)^2\right)}, \tag{33}$$

where n is number of time steps between the first and last position. $x_{\mathrm{Obs.}}$ and $y_{\mathrm{Obs.}}$ are longitudinal and lateral position observed. $x_{\mathrm{Mod.}}$ and $y_{\mathrm{Mod.}}$ are longitudinal and lateral position predicted by the model.

After the RMSE is computed for each trajectory individually, the total RMSE is computed as the root mean square of the individual RMSEs:

$$\mathrm{RMSE}_{\mathrm{Total}} = \sqrt{\frac{1}{n}\sum_{i=1}^{n}\left(\mathrm{RMSE}_{\mathrm{Trajectory}}\right)^2}, \tag{34}$$

where n is the number of mergers in the trajectory datasets. To avoid parameter sets that lead to collisions between the merger and vehicles in the main lane, these parameter sets are penalized by multiplying the total RMSE with $(n_{\mathrm{Coll}} + 1)$, where n_{Coll} is the number of collisions.

The total RMSE is minimized using the pattern search algorithm. To obtain realistic model parameters, the boundary conditions listed in Table 4 are applied. Since two datasets with different speed limits are used for the calibration, the maximum desired speed $v_{\max}$ is not calibrated. Instead, $v_{\max}$ is estimated based on the speed limits, which are 80 km/h = 22.22 m/s for the first dataset and 120 km/h = 33.33 m/s for the second dataset. For the second dataset, the maximum speed of trucks is set to 80 km/h and the speed of buses is set to 100 km/h. For mergers that exceed the speed limit, the individual $v_{\max}$ is set to the maximum observed speed of this vehicle.

The calibration of the model for the followers of mergers (submodel 2, Section 2.6) is conducted in a similar way. Followers that make a courtesy lane change are not considered in the calibration process due to the focus on the car-following behavior. Followers that follow the merger with a headway larger than 3 s are also not considered as they are likely not influenced by the merger. Since the followers do not change lanes themselves, the lane change duration τ_{LC} is not calibrated again; instead, the result of the calibration for mergers is used. The minimum DRAC to start the lane change is not contained in the model for the followers. The other model parameters are the same as for the mergers, and the same bounds (see Table 4) are applied. As an initial condition, we use the speed and position of the follower at the time when the merger is at the start of the on-ramp. We assume that the trajectory of the merger is known and that the behavior of the follower does not influence the behavior of the mergers. The trajectory of the follower is predicted by the model until the merger reaches the end of the on-ramp. The RMSE is defined as in equations (33) and (34), but without the term containing y because the lateral position of the follower is not relevant.

For the calibration of the regular car-following model (submodel 3, Section 2.1), the main difference to the first two cases is that we only consider vehicle pairs for which neither leader nor follower made a lane change in the whole road section included in the trajectory data. As an initial condition, we use the first available data point where both leader and follower are within the road section. The trajectory of the follower is predicted by the model until the leader leaves the road section. Parameter combinations that lead to a collision due to numerical instability if the leader suddenly brakes with $a_{\min}$ are excluded.

3.3. Simulation-Based Validation. To validate that the proposed model describes lane changes at on-ramps appropriately both at the microscopic and macroscopic scale, we set up traffic simulations of the two on-ramp locations described in Section 3.1. We use the open source traffic simulation software SUMO [40]. The car-following behavior and the lane change behavior at the on-ramps are modified according to the models presented in Section 2. The models are implemented in MATLAB [41], and the resulting vehicles' positions and speeds are transferred between MATLAB and SUMO with SUMO's traffic control interface (TraCI). Desired and courtesy lane changes are handled by SUMO itself. The traffic demand is taken from the trajectory data by aggregating the number of vehicles on the on-ramp and in the main lanes in intervals of 1 minute. For the first location (Duisburg), we distinguish four vehicle categories (car, van, truck, and bus), while the data for the second location (Cologne) only distinguish three vehicle categories (car, van, and truck). The maximum speed of the vehicles is set slightly above the speed limit (86 km/h for the first location with a speed limit of 80 km/h and 130 km/h for the second location with speed limit of 120 km/h), which corresponds to typical driving behavior in Germany. At the second location, buses and trucks have a lower maximum speed of 105 km/h and 86 km/h, respectively. For simplicity, we assume that the other model parameters have the same values for all vehicle categories.

To achieve a small deviation between simulated and observed traffic on macroscopic scale, the simulation should yield the same amount of congested traffic (i.e., similar average speeds) as the trajectory data. However, the congested traffic in both trajectory datasets originates not only from the on-ramps but also from bottlenecks outside the range of the datasets. Since these bottlenecks are not contained in the simulation either, the amount of congestion occurring in the simulation would be smaller than in reality. To account for the bottlenecks in the simulation, the speed limit at the downstream end of the simulated road section is changed dynamically according to the observed average speed at the downstream end of the road section contained in the trajectory data.

Table 4: Lower and upper bounds of the model parameter values.

Model parameter	Lower bound	Upper bound
Maximum speed v_{max}	(Not calibrated)	(Not calibrated)
Maximum acceleration a_{max}	1.0 m/s^2	3.0 m/s^2
Minimum acceleration a_{min}	−10.0 m/s^2	−3.0 m/s^2
Minimum distance at standstill Δx_{min}	1.0 m	7.0 m
Desired headway T_{des}	0.5 s	2.0 s
Lane change duration τ_{LC}	3.0 s	6.0 s
Minimum DRAC to start lane change $DRAC_{min}$	−1.5 m/s^2	−0.1 m/s^2

4. Results and Discussion

In this section, we present the results of the model calibration and validation and discuss the capabilities and limitations of the model.

4.1. Calibration Results. Table 5 shows the calibrated parameters of the lane change model for mergers. The calibration yields reasonable values for both locations. The values of a_{max} are equal to the lower bound, which indicates that mergers do not require large accelerations to reach the desired headway. The values of τ_{LC} are equal to the upper bound, which indicates that the average lane change duration is larger than 6 s. However, it must be noted that the definition of the lane change start time is not straightforward in the trajectory data because vehicles do not drive exactly in the center of the lanes. The lower value of $DRAC_{min}$ for the Duisburg dataset shows that mergers accept riskier situations when they start their lane change. A possible explanation for this observation could be the smaller length of the on-ramp. In the Cologne dataset, the values of both a_{min} and Δx_{min} are equal to one of the bounds. This is presumably a calibration artifact due to the small speed variation in the data. The RMSE values for calibration and validation are in the same order of magnitude, which shows that the model is not overfitted to the data.

Table 6 shows the calibrated parameters of the model for the followers of mergers. The desired headway of the followers is larger compared to the mergers. However, the desired headway only refers to the end of the lane change, while smaller headways are possible during the lane change when the merger accelerates. The values of a_{max} and Δx_{min} are equal to the lower bounds, which indicates that the data do not contain situations where the follower accelerated more or where the follower came to a standstill. For the Cologne dataset, the RMSE of the validation data is slightly larger than the RMSE of the calibration data. A possible explanation for this difference is that only the validation data contain congested traffic and that the model has been slightly overfitted to uncongested traffic. For the Duisburg dataset, there is no significant difference between the two RMSE values because both parts of the trajectory data contain congested traffic.

Table 7 shows the calibrated parameters of the car-following model based on desired headways. The values of T_{des} are similar to the values of T_{des} for the followers of mergers and they are larger than the values of T_{des} for the mergers. This difference shows that mergers intend to increase their headway after the merge when they approach regular car-following behavior. Thus, the model implicitly accounts for relaxation.

In general, the calibration results show that the microscopic calibration methodology, which is established for car-following models, is also applicable to lane change models. Nevertheless, it is important that the trajectory data used for calibration contain congested traffic conditions in order to obtain reasonable parameter values that are also valid for these conditions.

4.2. Sensitivity Analysis. To analyze how the choice of the parameter values affects the error of the calibration, we conduct a sensitivity analysis in which we vary the calibrated parameter values by +10 and −10% and compare the resulting prediction errors with the prediction error of the calibrated parameters. Ideally, the prediction error should increase in both directions if the parameters are successfully calibrated.

Table 8 shows that the errors change by less than 1% in most cases, which indicates that the calibration methodology is robust. This finding is particularly relevant for the practical application of the model in traffic simulations, in which it is not always feasible to thoroughly calibrate the parameters. In some cases, the error decreases if the calibrated value is varied. This occurs either if the varied value is outside the defined bounds or if the optimization algorithm converges to a solution slightly off the global minimum. Which parameter is the most sensitive depends on the model and on the dataset. Overall, a_{min} and Δx_{min} are the least sensitive parameters, and T_{des} and τ_{LC} are the most sensitive parameters.

4.3. Example Cases. To understand the behavior of the lane change model and to analyze its strengths and limitations, we extract three example cases from the trajectory data that represent typical merging situations:

1. Merger is slower than main lane traffic and selects the current leader
2. Merger is slower than main lane traffic and is passed
3. Merger is faster than main lane traffic and passes

Figure 6 and Table 9 show the positions and speeds of the merger and the three closest potential leaders and followers in the moment when the merger is at the start of the on-ramp. Table 9 also shows the results of the model in the three example cases.

Table 5: Calibrated model parameters of the lane change model for mergers.

Parameter	Duisburg dataset	Cologne dataset
Maximum speed v_{max}	80 km/h*	120 km/h*
Maximum acceleration a_{max}	1.00 m/s^2	1.00 m/s^2
Minimum acceleration a_{min}	−4.00 m/s^2	−10.00 m/s^2
Minimum distance at standstill Δx_{min}	2.48 m	7.00 m
Desired headway T_{des}	0.80 s	0.65 s
Lane change duration τ_{LC}	6.00 s	6.00 s
Minimum DRAC to start lane change $DRAC_{min}$	−1.50 m/s^2	−0.10 m/s^2
RMSE calibration data	3.60 m	5.49 m
RMSE validation data	3.16 m	5.14 m

*Not calibrated.

Table 6: Calibrated model parameters of the model for followers of mergers.

Parameter	Duisburg dataset	Cologne dataset
Maximum speed v_{max}	80 km/h*	120 km/h*
Maximum acceleration a_{max}	1.00 m/s^2	1.00 m/s^2
Minimum acceleration a_{min}	−3.00 m/s^2	−3.88 m/s^2
Minimum distance at standstill Δx_{min}	1.00 m	1.00 m
Desired headway T_{des}	1.40 s	1.02 s
RMSE calibration data	3.97 m	5.41 m
RMSE validation data	3.99 m	8.59 m

*Not calibrated.

Table 7: Calibrated model parameters of the car-following model.

Parameter	Duisburg dataset	Cologne dataset
Maximum speed v_{max}	80 km/h*	120 km/h*
Maximum acceleration a_{max}	1.00 m/s^2	1.16 m/s^2
Minimum acceleration a_{min}	−6.95 m/s^2	−8.78 m/s^2
Minimum distance at standstill Δx_{min}	1.00 m	1.00 m
Desired headway T_{des}	1.30 s	1.12 s
RMSE calibration data	6.71 m	10.02 m
RMSE validation data	6.31 m	11.04 m

*Not calibrated.

In Case 1, the model predicts correctly that the merger selects the current leader because the merger cannot pass and cannot be passed (see Table 9). If the merger decided to be passed, it would have to decelerate with $a_M = -0.47$ m/s^2 according to the model, and it would take $\tau_E = 14.6$ s to reach the end of the on-ramp ($x_E = 409$ m). Since the lane change takes $\tau_{LC} = 6.0$ s, the available time to be passed is $\tau_{Pass} = 8.6$ s. After this time, the merger reaches $x_M = 368.7$ m. Within the same time, the potential leader reaches $x_L = 375.0$ m, so the gross gap is 6.3 m. Since both vehicles are approximately 5 m long, the net gap between merger and potential leader is smaller than the minimum gap of $\Delta x_{min} = 2.48$ m (Duisburg dataset, see Table 5). This means the merger cannot be passed. If the merger decided to pass, it would have to accelerate with $a_M = 0.53$ m/s^2. The merger would then reach $x_M = 350.5$ m within the available time to pass ($\tau_{Pass} = 4.2$ s). However, the potential follower is still in front of the merger ($x_F = 366.9$ m) after this time. This means the merger cannot pass either. As a result, the model predicts that the merger selects the current gap. Even if passing or being passed were possible, the merger would still select the current gap because it is the gap with the largest difference Δa between the required acceleration to stay behind the leader (a_M) and the required acceleration to stay in front of the follower ($a_{M,Fol}$).

Figure 7 (left) shows the predicted trajectory and the observed trajectory of the merger, leader, and follower in Case 1 during the whole merging process. It is evident that the calibrated value for the desired headway ($T_{des} = 0.80$ s) is smaller than the observed desired headway, which results in a deviation in the longitudinal direction ($RMSE_X = 5.49$ m). Since the model assumes the same parameter values for each driver, this deviation is inevitable. The lateral position, however, can be predicted very accurately in this example case ($RMSE_Y = 0.30$ m). Furthermore, it is worth noting that both the predicted and the observed acceleration of the merger change along the on-ramp. If the assumption that the vehicles in the main lane maintain their speed was valid, the model would predict a constant acceleration along the on-ramp. However, both the leader and the follower continuously adapt their speed depending on their own leaders. As a result, the acceleration of the merger also adapts. The model is able to reflect this continuous adaptation.

Table 8: Sensitivity analysis of the calibrated model parameters.

Parameter		Duisburg dataset		Cologne dataset	
		RMSE change for calibrated value + 10%	RMSE change for calibrated value −10%	RMSE change for calibrated value + 10%	RMSE change for calibrated value −10%
Merger	Maximum acceleration a_{max}	+0.26%	−0.35%*	+5.94%	−5.46%*
	Minimum acceleration a_{min}	−0.01%	−0.02%	0.00%*	0.00%
	Minimum distance at standstill Δx_{min}	−0.15%	−0.05%	−0.21%*	−0.37%
	Desired headway T_{des}	+1.55%	+2.14%	−0.07%	+0.58%
	Lane change duration τ_{LC}	+1.68%*	+6.54%	−4.66%*	+3.28%
	Minimum DRAC to start lane change $DRAC_{min}$	0.00%*	0.00%	+3.94%	0.00%*
Followers of mergers	Maximum acceleration a_{max}	+0.21%	−0.25% *	+1.75%	−2.22%*
	Minimum acceleration a_{min}	+0.82%	−0.21%*	0.00%	0.00%
	Minimum distance at standstill Δx_{min}	+0.10%	−0.04%*	+0.07%	−0.04%*
	Desired headway T_{des}	+1.46%	+1.36%	+0.75%	+0.60%
Car-following	Maximum acceleration a_{max}	+0.47%	−0.46%*	+0.12%	+0.16%
	Minimum acceleration a_{min}	+0.01%	**	+0.40%	**
	Minimum distance at standstill Δx_{min}	+0.07%	−0.04%*	+0.29%	−0.25%*
	Desired headway T_{des}	+2.34%	**	+6.11%	**

*The value lies outside the bounds for this parameter.
**Model becomes numerically unstable with these parameter values.

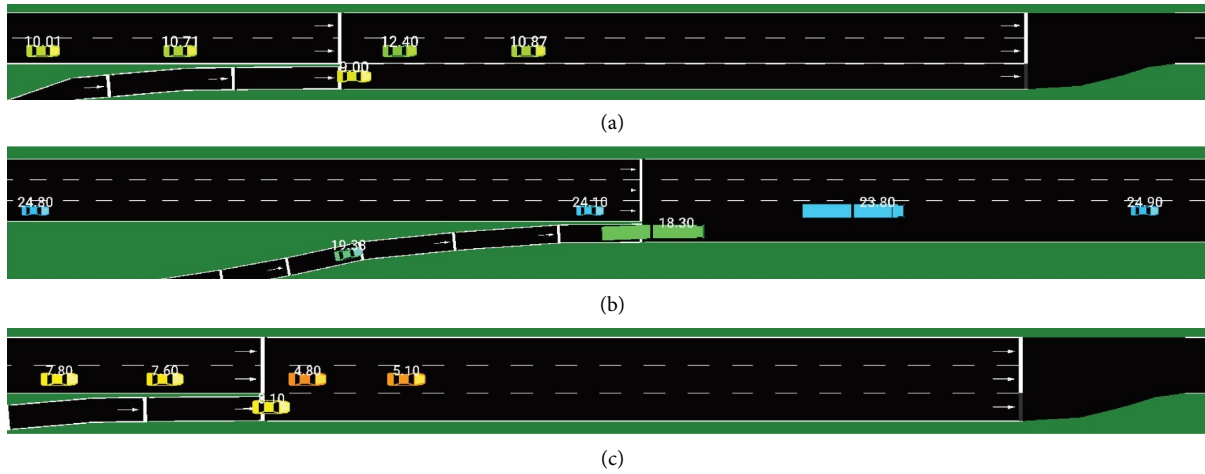

FIGURE 6: Example cases for merging at on-ramps. The color of the vehicles and the numbers above the vehicles indicate the current speed of the vehicles. (a) Case 1: merger is slower than main lane traffic and selects the current leader, (b) Case 2: merger is slower than main lane traffic and is passed, (c) Case 3: merger is faster than main lane traffic and passes.

TABLE 9: Initial conditions and results of the lane change model for the three example cases (see Figure 6).

Case	x_M	v_M	x_L	v_L	x_F	v_F	a_M	$a_{M,\text{Fol.}}$	Δa	τ_E	τ_{Pass}	x_M after pass	x_L after pass	x_F after pass	Passing possible	Selected leader
			282.5	10.7	262.0	10.0	−0.47	−0.09	−0.38	14.6	8.6	368.7	375.0	348.4	No	
1	308.6	9.0	315.4	12.4	282.5	10.7	0.45	0.13	0.31	10.5	—	—	—	—	—	Yes
			334.6	10.9	315.4	12.4	0.53	1.08	−0.55	10.2	4.2	350.5	379.8	366.9	No	
			103.5	24.1	2.5	24.8	0.18	0.16	0.01	13.2	7.2	259.0	277.5	182.1	No	
2	121.7	18.3	158.2	23.8	103.5	24.1	0.85	1.04	−0.19	11.5	5.5	—	—	—	—	Yes
			204.5	24.9	158.2	23.8	1.0	2.09	−1.10	11.2	5.2	230.0	333.7	281.2	No	
			293.1	7.6	278.7	7.8	−0.33	−0.09	−0.24	19.0	13.0	384.6	391.6	380.7	No	
3	307.6	8.1	312.5	4.8	293.1	7.6	−0.35	−0.06	−0.29	25.3	—	—	—	—	—	Yes
			325.9	5.1	312.5	4.8	−0.29	−0.21	−0.08	21.6	15.6	398.4	405.4	388.0	No	

In Case 2, the merger is very close to the current follower at the start of the on-ramp (see Figure 6(b)). Due to the speed difference to the current follower, the merger is not able to stay in the current gap. Instead, the current follower passes the merger and becomes its leader. According to the model, however, the merger cannot be passed within $\tau_{\text{Pass}} = 8.6$ s because the gross gap between merger and potential leader ($x_L - x_M = 18.5$ m) is too small given the length of the merger (ca. 18 m) and the minimum gap ($\Delta x_{\min} = 7.0$ m for the Cologne dataset) (see Table 9). The model instead predicts that the merger intends to stay in the current gap and accelerates with $a_M = 0.85\,\text{m/s}^2$. After approximately 4 s, the initial follower passes the merger, which means that the current gap changes (see Figure 7 center). At this moment, the model predicts that the merger must stay in the new current gap. To stay behind the new leader, the merger must decelerate according to the model. This example shows that the model is able to correct its initially incorrect decision. However, this correction results in a sudden acceleration change. The RMSE in longitudinal direction ($\text{RMSE}_X = 5.79$ m) is in the same order of magnitude as in the first example case, although the deviation in the acceleration is larger than in the first example case. The RMSE in lateral direction ($\text{RMSE}_Y = 1.11$ m) is larger than in the first example case because the model predicts a later lane change start. Again, the assumption that the parameter values are the same for each driver affects the prediction accuracy of the model. For example, if $\Delta x_{\min}$ or τ_{LC} were smaller in this example case, the model would predict that the merger can be passed, and the deviation both in longitudinal and in lateral direction would be smaller.

In Case 3, the traffic in the main lane is congested and the merger has a larger initial speed than the traffic in the main lane (see Figure 6(c)). As a result, the merger passes its current leader, and the current leader becomes the follower. According to the model, however, passing is not possible because the gross gap between merger and potential leader ($x_L - x_M = 7.0$ m) is too small given the lengths of the vehicles (ca. 5 m) and the minimum gap ($\Delta x_{\min} = 2.48$ m for the Duisburg dataset) (see Table 9). Nevertheless, the merger passes the current leader after approximately 2 s due to the small absolute value of a_M and the large speed difference between merger and current leader (see Figure 7 right). At this moment, the model predicts that the merger must stay

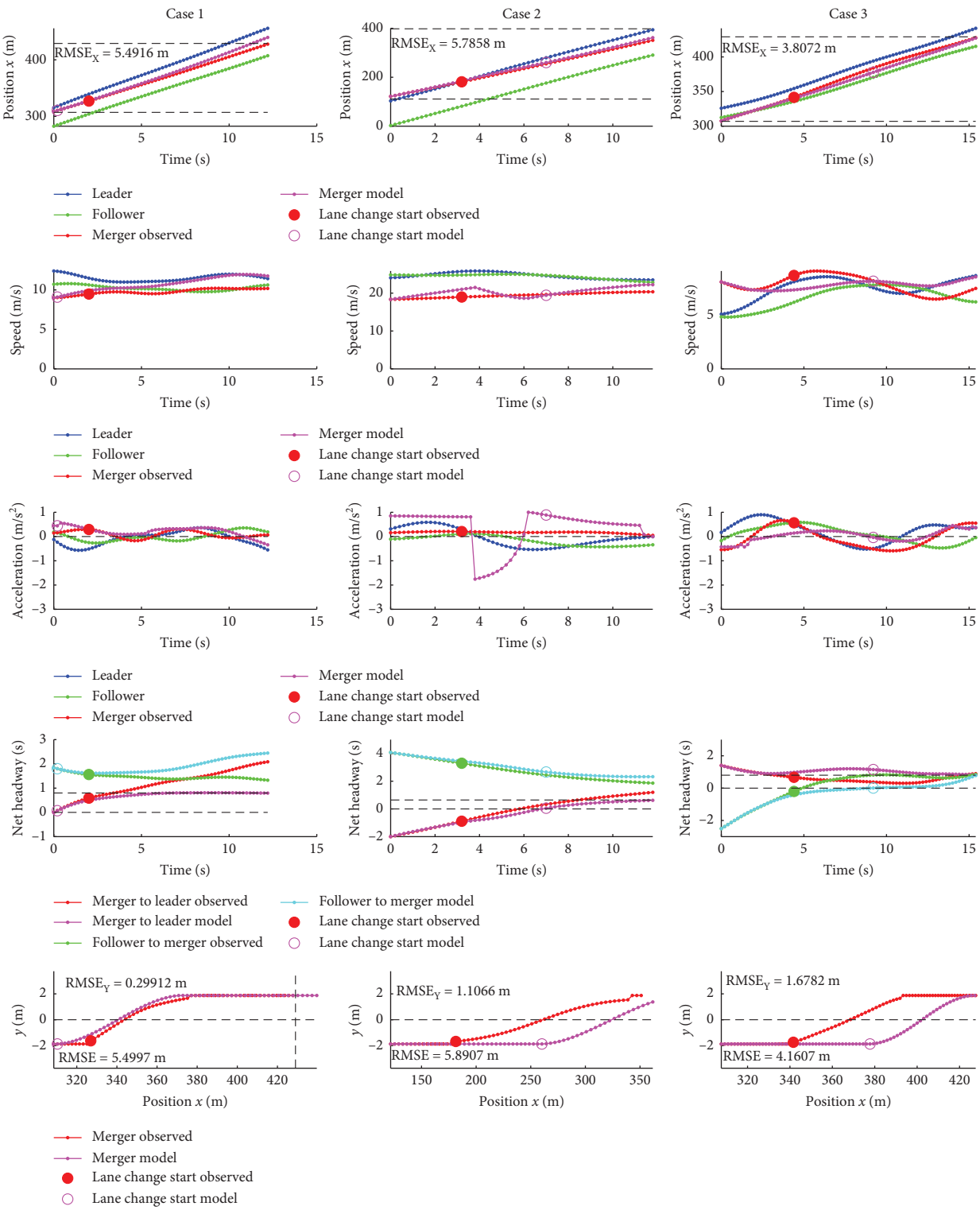

Figure 7: Trajectories of merger (observed and predicted by the model), leader, and follower in the three example cases shown in Figure 6.

in the new current gap. This leads to a discontinuity in the acceleration, but the discontinuity is much smaller than in example case 2. The RMSE in the longitudinal direction (RMSE$_X$ = 3.81 m) mainly results from the fact that the observed net headway between merger and leader is very small well after the lane change start. This unsafe behavior is not considered in the model. Instead, the model predicts that the net headway between merger and leader converges to the desired headway (T_{des} = 0.80 s for the Duisburg dataset) without falling below it. In return, the predicted net headway

between merger and follower is smaller. However, it must be noted that we use the observed trajectory of the follower to compute the headway, which means the follower does not react to the modeled trajectory.

The three example cases show that the model has a good capability of predicting the correct leader even if the prediction is wrong at the start of the on-ramp. The reason behind this wrong prediction is the condition that the gap must be non-negative after passing (equations (26) and (27)). This condition is necessary to prevent impossible passing maneuvers, but it also prevents some possible passing maneuvers because it might lead to safer merging behavior than observed in the trajectory data. If only the condition that the selected gap has the largest difference between a_M and $a_{M,\mathrm{Fol}}$ is considered, the model predicts the selected gap correctly in all three example cases. To analyze whether this observation holds for all observed merging maneuvers, we present a more generalized analysis of the leader selection in Section 4.4.1.

The three example cases also indicate that the model would make better predictions if other parameter values were used. However, the calibrated parameters are deterministic and represent average driving behavior. For future applications of the model in traffic simulations, stochastic parameters are expected to yield more realistic results.

4.4. Validation Results. For the validation results presented in this section, we use the part of the trajectory data presented in Section 3.1 that has not been used for calibration, as well as the results of the traffic simulations described in Section 3.3.

4.4.1. Leader Selection. To analyze how well the lane change model is able to predict which vehicle the merger selects as a leader, we use a confusion matrix (see Table 10). The model predicts a leader at every timestep until the lane change start, but the tables contain only the prediction at the start of the on-ramp (Table 10 top) and at the start of the lane change (Table 10 bottom). Table 10 confirms the observations made in Section 4.3 that the model is not always able to predict the selected leader correctly at the start of the on-ramp. Cases in which the merger passes are predicted as "no passing" or rarely as "merger is passed." Cases in which the merger is passed are predicted correctly in the Cologne dataset, but rarely predicted as "no passing" in the Duisburg dataset. However, the model is always able to predict the selected leader correctly at the moment the lane change starts. This result shows that minimizing the RMSE in the longitudinal direction is a suitable approach to calibrate the leader selection component of the model. However, a major limitation of this analysis is that the trajectories of the potential leaders and followers do not adapt to the modeled trajectory of the merger. To overcome this limitation, we also analyze the number of passing mergers and mergers being passed in the simulations and compare these numbers with the trajectory data (see Section 4.4.3).

4.4.2. Lane Change Position. To validate the component of the model that predicts the lane change start time, we compare the observed and the modeled lane change positions (see Figure 8). Since the lane change start is not well defined for the trajectory data, we use the middle of the lane change as a reference, that is, the moment when the center of the vehicle crosses the marking between on-ramp and main lane. Figure 8 shows that there is a good agreement between the observed and modeled lane change positions in the Duisburg dataset, while there is no clear correlation in the Cologne dataset.

Figure 8(b) right indicates that the modeled lane change positions fall into two clusters, one cluster around $x \approx 200$ and the other cluster at $x > 260$. The reason for this behavior is that the merger can start the lane change in one of two cases. The first case is that the time until the end of the on-ramp equals the lane change duration ($\tau_E = \tau_{\mathrm{LC}}$). These lane changes occur mostly toward the end of the on-ramp ($x > 260$). The second case is that it is safe to start the lane change earlier ($\mathrm{DRAC} \leq \mathrm{DRAC}_{\mathrm{min}}$). Since the traffic density is low in the Cologne dataset, this condition is often fulfilled when mergers are at the start of the on-ramp, which leads to the cluster around $x \approx 200$. The observed lane change positions, however, are mostly between $x = 200$ and $x = 270$, which is between the two clusters. The most likely explanation for this deviation is the large length of the on-ramp in Cologne. Due to the length, mergers do not start the lane change early even it would be safe to do so. Instead, they remain on the on-ramp longer and reduce the speed difference to the vehicles in the main lane before they start the lane change. To reflect this behavior in the model, $\mathrm{DRAC}_{\mathrm{min}}$ would have to vary along the on-ramp so that mergers accept a larger accident risk toward the end of the on-ramp. However, this adaptation would increase the complexity of the model.

4.4.3. Microscopic Simulation Results. So far, we have compared observed trajectories with the corresponding modeled trajectories. While this approach is important to evaluate the model microscopically, it has several important limitations. One major reason for deviations between observed and modeled trajectories is the assumption that all drivers share the same model parameters. Another reason is the assumption that the follower of the merger does not adapt to the modeled trajectory of the merger. Furthermore, the behavior of the model cannot be analyzed in situations that are not included in the data. A traffic simulation can give insights into whether these limitations are relevant.

First, we analyze the number of mergers who pass or are passed by vehicles in the main lane. In the simulation, the follower of the merger adapts to the merger, which addresses one of the mentioned limitations. Table 11 shows that there is a good agreement between simulation and trajectory data for the Cologne dataset. There are slightly less passing maneuvers in the simulation than in reality, although the total number of passing maneuvers is small. The simulation of the Duisburg dataset contains considerably more situations where the merger passes vehicles in the main lane than

Table 10: Confusion matrix of the leader selection model.

	Duisburg				Cologne			
		Observed				Observed		
	Model	Merger is passed	No passing	Merger passes	Model	Merger is passed	No passing	Merger passes
Start of on-ramp	Merger is passed	4.2%	4.2%	1.0%	Merger is passed	4.0%	—	—
	No passing	1.0%	76.7%	11.5%	No passing	—	88.0%	8.0%
	Merger passes	—	—	—	Merger passes	—	—	—
		Observed				Observed		
	Model	Merger is passed	No passing	Merger passes	Model	Merger is passed	No passing	Merger passes
Start of lane change	Merger is passed	5.2%	—	—	Merger is passed	4.0%	—	—
	No passing	—	82.3%	—	No passing	—	88.0%	—
	Merger passes	—	—	12.5%	Merger passes	—	—	8.0%

Note: (left column) Duisburg dataset, (right column) Cologne dataset, (top) observed leader selection vs leader selection predicted at the start of the on-ramp, (bottom) observed leader selection vs leader selection predicted at the start of the lane change.

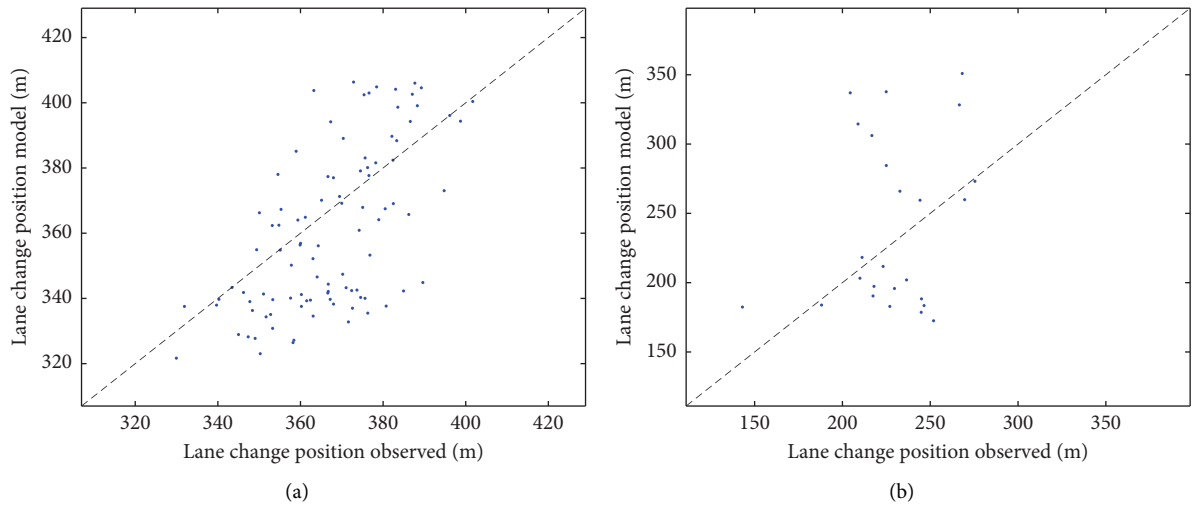

Figure 8: Comparison of the observed and modeled lane change positions. (a) Duisburg dataset, (b) Cologne dataset.

the trajectory data. Whether the merger decides to pass depends mainly on the speed difference to the vehicles in the main lane. In the Duisburg dataset, the mean speed in the main lane is small, which means that mergers are usually faster than vehicles in the main lane when they enter the on-ramp. In reality, it can be observed that mergers already adapt to the speed in the main lane before they enter the on-ramp. This early adaptation cannot be fully captured in the simulation. As a result, the speed difference in the simulation is often larger than in reality, which leads to more mergers passing vehicles in the main lane. A possible solution to overcome this limitation is to analyze the speed of the mergers before the on-ramp to identify the location where the mergers start to adapt to vehicles in the main lane.

Another important aspect of the merging behavior is the headway between the merger and the leader, which is controlled by the merger, and the headway between the merger and the follower, which is controlled by the follower. The most important difference between simulation and observation is that there are almost no negative headways at the start of the lane change in the simulation (see Figure 9). Negative headways are not inherently unsafe because the vehicles are not in the same lane yet and the headway usually increases after the lane change starts due to the speed difference between the two vehicles. Nevertheless, the model does not reproduce this risky behavior. To reflect this behavior, the model could be adapted by decreasing the lower bound of $\Delta x_{\min}$ to negative values, which would allow risky lane changes that start with negative gaps.

At the end of the lane change, there are some small headways in the data, which the model does not reproduce. As a result, the peak in the distribution in the simulation is at larger headways. Since the model assumes the same value of T_{des} for all mergers, the variation of the headway at the lane change end is smaller than in reality. A more realistic distribution of net headways could be achieved by using stochastic values of T_{des}. Nevertheless, this deterministic model generates varying headways due to the varying boundary conditions, in particular speed changes of the leader during the merging process. Apart from these mentioned differences, the model is able to reproduce the headway distributions well.

The third aspect of merging behavior is the speed difference between merger and the vehicles in the main lane. In the trajectory data of the Duisburg dataset, most mergers are slightly slower than the leader, but slightly faster than the follower (see Figure 10(a)). This tendency is also visible in the simulation, although larger (absolute) speed differences occur more often. Together with the headway distributions, these results indicate that real drivers temporarily accept small headways if the (absolute) speed difference is small, while the model aims for larger headways, which can only be reached if the (absolute) speed difference temporarily increases.

For the Cologne dataset, the deviation between simulation and observation is smaller (see Figure 10(b)). While the simulation yields a larger variation of speed differences between merger and leader at the end of the lane change compared to the trajectory data, the opposite is true for the speed differences between merger and follower at the start of the lane change. These results must be interpreted cautiously due to the different lane change positions (see Section 4.4.2).

4.4.4. Macroscopic Simulation Results. The microscopic evaluations presented so far do not give insights whether the model is able to describe traffic flow at the macroscopic scale. To evaluate the capability to reproduce the formation and propagation of congestion waves, we compare the speeds in the main lane as a function of time and position (see Figure 11). Since there is only a short period of congestion in the Cologne dataset, only the Duisburg dataset is analyzed. In both speed contour plots in Figure 11, it is evident that the on-ramp acts as a bottleneck, which means that there are lower speeds before the on-ramp ($x < 300$) than behind the on-ramp ($x > 430$). Thus, the lane change model accurately describes the traffic flow characteristics of the on-ramp. However, the speeds in the simulation before and behind the

Table 11: Comparison between simulation and observed trajectory data with respect to passing maneuvers.

Selected gap	Duisburg		Cologne	
	Simulation	Observed	Simulation	Observed
Merger is passed	4 (1.5%)	8 (3.1%)	10 (1.7%)	13 (2.2%)
No passing	164 (62.1%)	198 (75.9%)	576 (97.0%)	555 (95.5%)
Merger passes	96 (36.4%)	55 (21.1%)	8 (1.3%)	13 (2.2%)

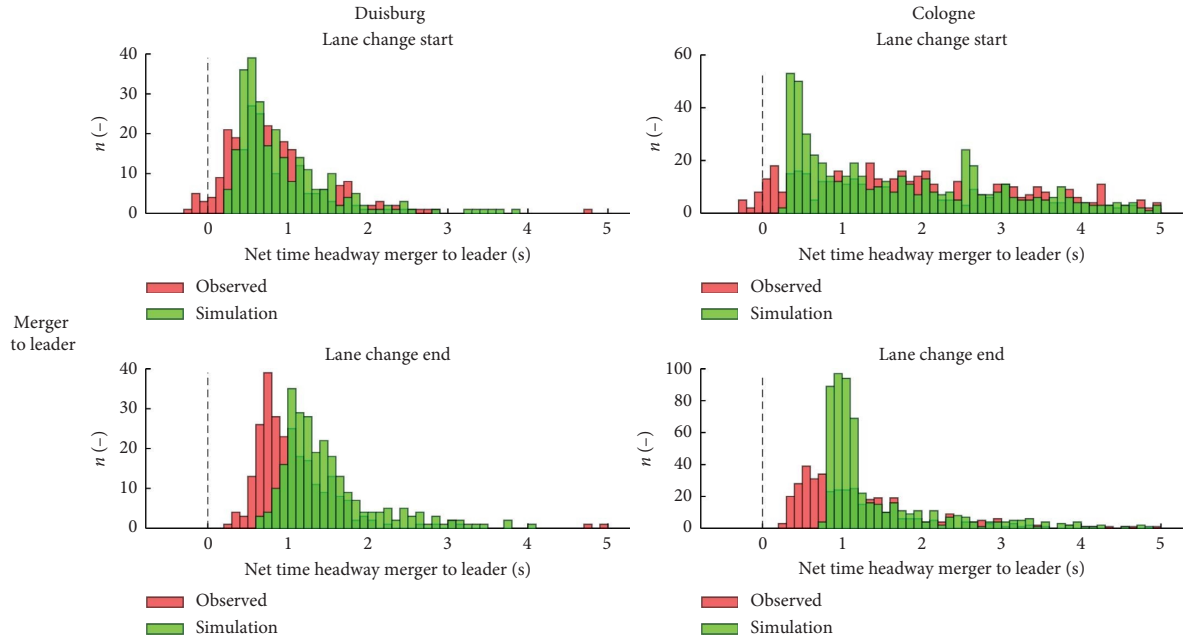

Figure 9: Distributions of headways at the start and at the end of the lane change. (a) Headway between merger and leader, (b) headway between merger and follower, (left) Duisburg dataset, (right) Cologne dataset.

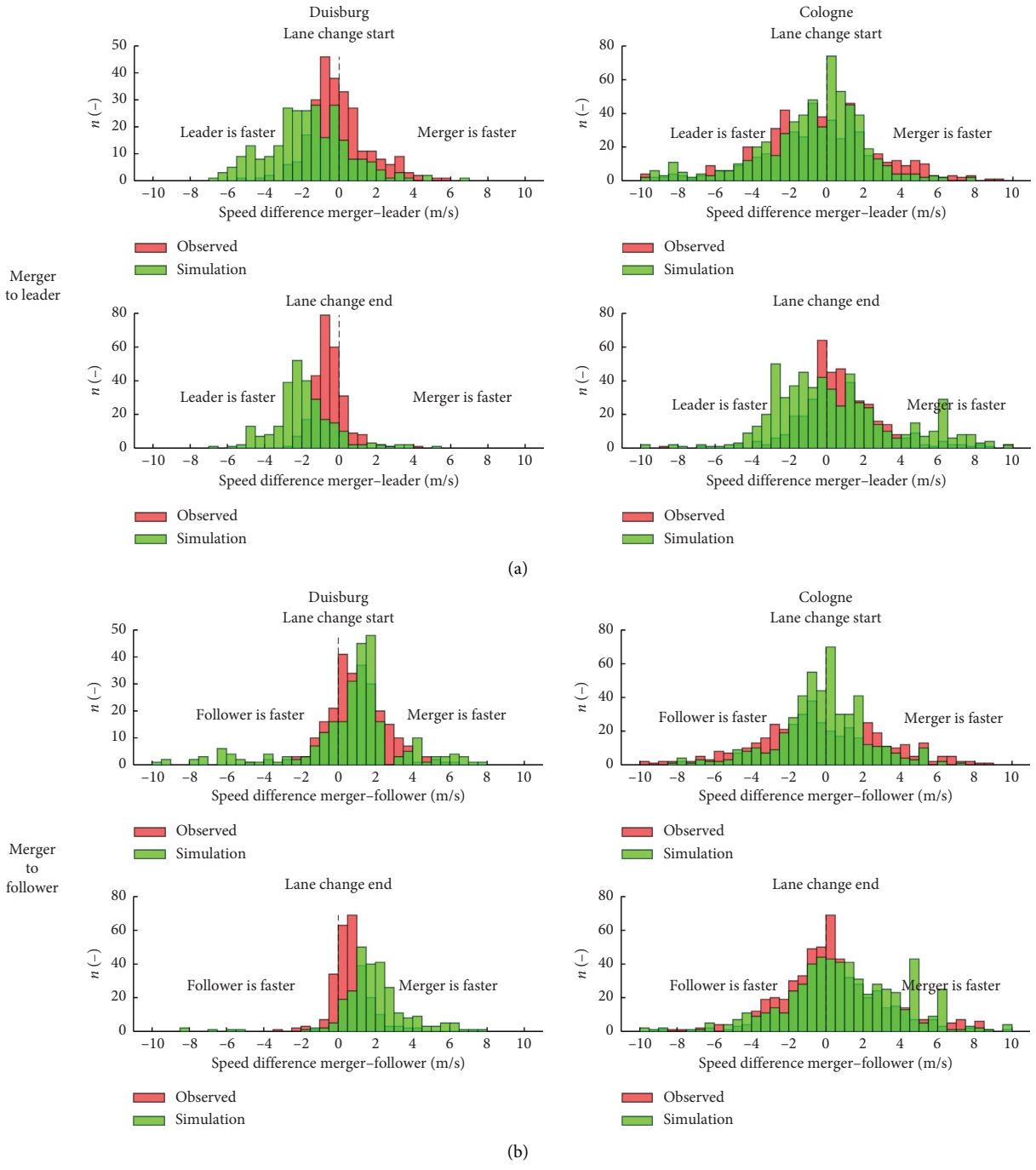

FIGURE 10: Distribution of speed differences at the start and at the end of the lane change. (a) Speed difference between merger and leader, (b) speed difference between merger and follower, (left) Duisburg dataset, (right) Cologne dataset.

on-ramp are slightly higher than in the data. This indicates that the car-following model overestimates the capacity of the freeway, which leads to less congestion. A possible explanation for these results could be the calibration methodology, in which we excluded a large proportion of the trajectories, mainly due to lane changes. It is conceivable that the trajectories used for calibration are not representative in terms of the car-following behavior. To represent the car-following behavior around the on-ramp better, a macroscopic calibration might be more suitable.

Figure 12 shows that the speed–density relationships of the main lane and the on-ramp can be reproduced accurately in the simulation. Only the few data points in the Cologne dataset with small speeds cannot be found in the simulation. The reason behind this is again that the capacity of the car-following model is overestimated. As a result, the congestion

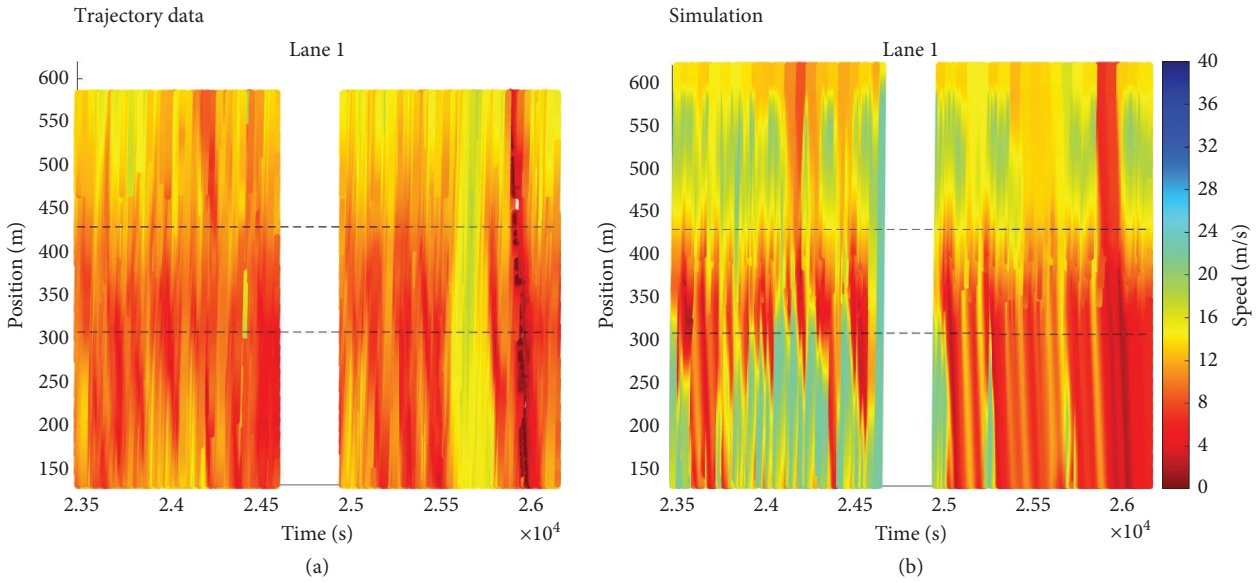

FIGURE 11: Speed contour plots for the main lane of the Duisburg dataset. (a) Trajectory data, (b) simulation. The dashed horizontal lines represent the start and end of the on-ramp.

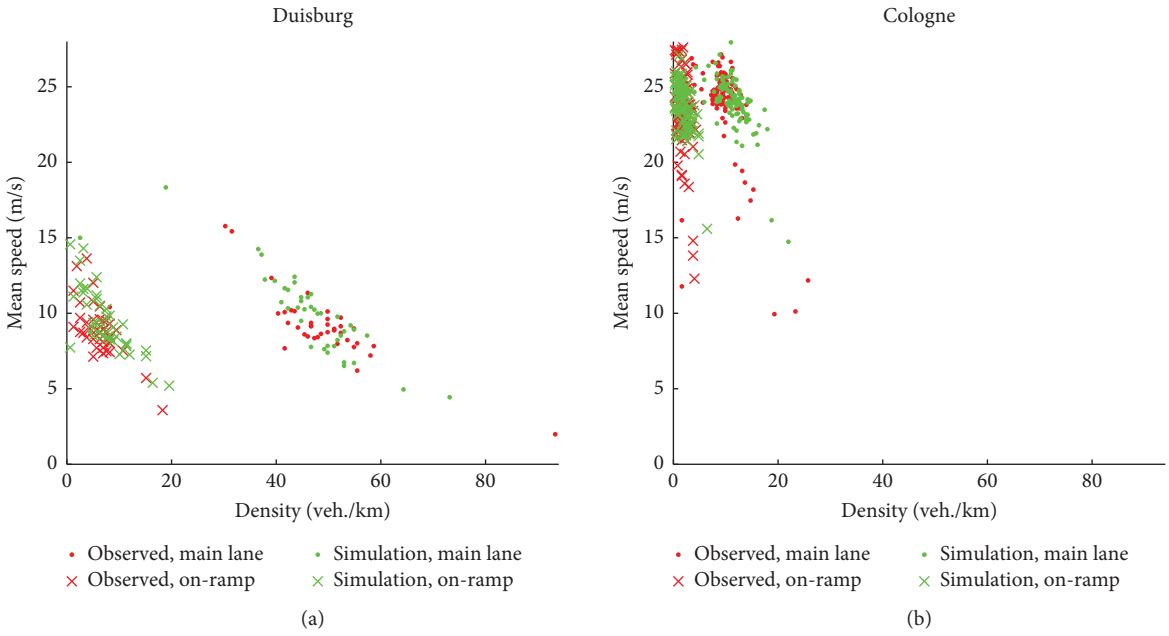

FIGURE 12: Speed–density relationship of main lane and on-ramp for the Duisburg dataset (a) and the Cologne dataset (b).

that originates from a bottleneck downstream does not propagate realistically. Nevertheless, the speed–density relationships show that the lane change model can represent the traffic flow at the on-ramp well.

5. Conclusions

In this paper, we presented a lane change model for freeway on-ramps derived from a car-following model based on desired time headways. The model consists of three submodels, one for merging vehicles, one for the followers of merging vehicles, and one for all remaining vehicles with regular car-following behavior. The trajectory-based calibration methodology was adopted from car-following models as well. The seven parameters of the model have an intuitive meaning, which enables an evaluation of the calibrated parameter values. The calibration results indicate that the parameter values are plausible and that the model predicts the trajectory of mergers with an RMSE of 3.6 m in the dataset with congested traffic and a short on-ramp and 5.5 m in the dataset with free-flow traffic and a longer on-ramp. The RMSE for the trajectory of the followers of mergers is in the same order of magnitude. The sensitivity analysis shows that parameter variation causes only a small

increase in RMSE, indicating that the calibration is robust. A detailed analysis of three typical cases (merger selects current leader, merger is passed, and merger passes) demonstrates that, despite the small number of parameters, the model can accurately represent the longitudinal driver behavior of mergers and their followers in the main lane, as well as the decision of the merger to pass or be passed. The lateral driver behavior, mainly the positions of the lane changes, can be described well only for the location with a short on-ramp and with congested traffic. In microscopic simulations, the number of mergers passing a vehicle in the main lane is slightly overestimated, which likely results from mergers adapting their speed to traffic in the main lane before the on-ramp—a behavior not fully captured in the simulation. The distribution of net time headways and speed differences is accurately represented in the simulation, except in cases involving risky behavior with very small headways at the start of the lane change. The lane change model makes good predictions also at the macroscopic scale in terms of the speed–density relationships and the role of the on-ramp as a bottleneck. However, the results indicate that the car-following model overestimates the capacity of the freeway before and behind the on-ramp, which impairs the capability of the model to reproduce the propagation of congestion. The main goal of the novel car-following model presented in this paper was to apply it to the car-following behavior of merging vehicles and their followers. Further research is required to improve the car-following model for regular car-following behavior.

For the validation of the model, a deterministic approach with the same parameter values for all drivers was used. Stochastic parameter values could further improve the results, in particular the headway distributions. However, a stochastic approach would require a more complex calibration methodology in order to identify the best parameter values for each individual driver.

With the three submodels, a complete traffic simulation of an on-ramp can be run, with the exception of desired and courtesy lane changes. Further research is recommended to evaluate whether the lane change model can be extended to these types of lane changes. We assume that the main concept of our lane change model, which is that the lane changing vehicle has two leaders and that it gradually reaches the desired headway after some time, is also applicable for desired and courtesy lane changes.

The validation results have shown that the model is suitable to assess on-ramps in terms of traffic flow. For example, the effect of the length of the on-ramp and the effect of different traffic volumes and different truck ratios can be analyzed. Whether the model is also able to assess on-ramps in terms of traffic safety, that is, the question whether the simulation yields a similar amount and similar spatial distribution of conflicts, is also a topic for further research. Since the model contains a SSM as a parameter, we expect that the model can also be optimized for traffic safety in addition to traffic flow in future research.

The model can also be used to assess traffic management measures related to on-ramps, for example, ramp metering. While current ramp-metering algorithms are mostly based on macroscopic parameters, our lane change model could be used to develop a microscopic ramp-metering algorithm.

While our model primarily describes human driving behavior, it also holds relevance in the context of connected and automated vehicles. Recent research explores how automated vehicles interact with human-driven vehicles, and which implications this mixed traffic has for both traffic flow and safety. To make valid predictions, models that capture the driving behavior of both humans and automated vehicles are essential.

Data Availability Statement

The data that support the findings of this study are available from the corresponding author upon reasonable request.

Conflicts of Interest

The authors declare no conflicts of interest.

Funding

The work presented in this paper is part of the project NeMo (Neue Ansätze der Verkehrsmodellierung unter Berücksichtigung komplexer Geometrien und Daten—New traffic models considering complex geometries and data) funded by Deutsche Forschungsgemeinschaft (DFG) (Grant no. 461365406).

Acknowledgments

The authors would like to thank Eszter Kalló, Michael Herty, and Niklas Kolbe from RWTH Aachen University for the valuable discussions throughout the project. The authors would also like to thank Mohamed Kastouri from RWTH Aachen University for his dedication in preparing and providing the trajectory data.

References

[1] V. Knoop, *Introduction to Traffic Flow Theory*, 2nd edition (Delft, Netherlands: Delft University of Technology, 2018).

[2] J. Erdmann, "SUMO's Lane-Changing Model," *Lecture Notes in Mathematics* (2015): 105–123, https://elib.dlr.de/102254/1/Springer-SUMOs_Lane_changing_model.pdf, https://doi.org/10.1007/978-3-319-15024-6_7.

[3] Z. Zheng, "Recent Developments and Research Needs in Modeling Lane Changing," *Transportation Research Part B: Methodological* 60, no. 8 (2014): 16–32, https://doi.org/10.1016/j.trb.2013.11.009.

[4] W. J. Schakel, V. L. Knoop, and B. van Arem, "Integrated Lane Change Model With Relaxation and Synchronization," *Transportation Research Record: Journal of the Transportation Research Board* 2316, no. 1 (2012): 47–57, https://doi.org/10.3141/2316-06.

[5] J. A. Laval and L. Leclercq, "Microscopic Modeling of the Relaxation Phenomenon Using a Macroscopic Lane-Changing Model," *Transportation Research Part B: Methodological* 42, no. 6 (2008): 511–522, https://doi.org/10.1016/j.trb.2007.10.004.

[6] H. Kita, "A Merging: Giveway Interaction Model of Cars in a Merging Section: A Game Theoretic Analysis,"

Transportation Research Part A: Policy and Practice 33, no. 3-4 (1999): 305–312, https://doi.org/10.1016/S0965-8564(98)00039-1.

[7] J. Wang, R. Liu, and F. Montgomery, "A Simulation Model for Motorway Merging Behaviour," in *Transportation and Traffic Theory: Flow, Dynamics and Human Interaction: Proceedings of the 16th International Symposium on Transportation and Traffic Theory* (Amsterdam, Boston: Elsevier, 2005), 281–302.

[8] A. van Beinum, E. Broekman, H. Farah, W. Schakel, F. Wegman, and S. Hoogendoorn, "Critical Assessment of Microscopic Simulation Models for Simulating Turbulence Around Motorway Ramps," *Journal of Transportation Engineering, Part A: Systems* 146, no. 2 (2020): 501, https://doi.org/10.1061/JTEPBS.0000296.

[9] D. Chen and S. Ahn, "Capacity-Drop at Extended Bottlenecks: Merge, Diverge, and Weave," *Transportation Research Part B: Methodological* 108 (2018): 1–20, https://doi.org/10.1016/j.trb.2017.12.006.

[10] K. Chen, Z. Li, P. Liu, V. L. Knoop, Y. Han, and Y. Jiao, "Evaluating the Safety and Efficiency Impacts of Forced Lane Change With Negative Gaps Based on Empirical Vehicle Trajectories," *Accident Analysis and Prevention* 203 (2024): 107622, https://doi.org/10.1016/j.aap.2024.107622.

[11] A. Kesting, M. Treiber, and D. Helbing, "General Lane-Changing Model MOBIL for Car-Following Models," *Transportation Research Record: Journal of the Transportation Research Board* 1999, no. 1 (2007): 86–94, https://doi.org/10.3141/1999-10.

[12] A. Kondyli and L. Elefteriadou, "Modeling Driver Behavior at Freeway: Ramp Merges," *Transportation Research Record: Journal of the Transportation Research Board* 2249, no. 1 (2011): 29–37, https://doi.org/10.3141/2249-05.

[13] F. Marczak, W. Daamen, and C. Buisson, "Merging Behaviour: Empirical Comparison Between Two Sites and New Theory Development," *Transportation Research Part C: Emerging Technologies* 36, no. 4 (2013): 530–546, https://doi.org/10.1016/j.trc.2013.07.007.

[14] C. Ng, S. Susilawati, M. A. S. Kamal, and I. M. L. Chew, "Development of a Binary Logistic Lane Change Model and Its Validation Using Empirical Freeway Data," *Transportation Business: Transport Dynamics* 8, no. 1 (2020): 49–71, https://doi.org/10.1080/21680566.2020.1715309.

[15] K. Kang and H. A. Rakha, "Game Theoretical Approach to Model Decision Making for Merging Maneuvers at Freeway On-Ramps," *Transportation Research Record: Journal of the Transportation Research Board* 2623, no. 1 (2017): 19–28, https://doi.org/10.3141/2623-03.

[16] C. F. Choudhury, "Modeling Driving Decisions With Latent Plans" (2007).

[17] R. Delpiano, J. C. Herrera, J. Laval, and J. E. Coeymans, "A Two-Dimensional Car-Following Model for Two-Dimensional Traffic Flow Problems," *Transportation Research Part C: Emerging Technologies* 114 (2020): 504–516, https://doi.org/10.1016/j.trc.2020.02.025.

[18] W. Schakel, V. Knoop, M. Keyvan-Ekbatani, and H. van Lint, "Social Interactions on Multi-Lane Motorways: Towards a Theory of Impacts" (2023).

[19] C. Dong, H. Wang, Y. Li, X. Shi, D. Ni, and W. Wang, "Application of Machine Learning Algorithms in Lane-Changing Model for Intelligent Vehicles Exiting to Off-Ramp," *Transportmetrica: Transportation Science* 17, no. 1 (2021): 124–150, https://doi.org/10.1080/23249935.2020.1746861.

[20] S. Mozaffari, M. A. Sormoli, K. Koufos, and M. Dianati, "Multimodal Manoeuvre and Trajectory Prediction for Automated Driving on Highways Using Transformer Networks," *IEEE Robotics and Automation Letters* 8, no. 10 (2023): 6123–6130, https://doi.org/10.1109/LRA.2023.3301720.

[21] X. Wan, P. J. Jin, F. Yang, J. Zhang, and B. Ran, "Modeling Vehicle Interactions During Merge in Congested Weaving Section of Freeway Ramp," *Transportation Research Record: Journal of the Transportation Research Board* 2421, no. 1 (2014): 82–92, https://doi.org/10.3141/2421-10.

[22] G. Bham, "A Simple Lane Change Model for Microscopic Traffic Flow Simulation in Weaving Sections," *Transportation Letters* 3, no. 4 (2011): 231–251, https://doi.org/10.3328/TL.2011.03.04.231-251.

[23] M. Treiber and A. Kesting, "Microscopic Calibration and Validation of Car-Following Models: A Systematic Approach," *Procedia-Social and Behavioral Sciences* 80, no. 10 (2013): 922–939, https://doi.org/10.1016/j.sbspro.2013.05.050.

[24] M. Berghaus, E. Kallo, and M. Oeser, "Car-Following Model Calibration Based on Driving Simulator Data to Study Driver Characteristics and to Investigate Model Validity in Extreme Traffic Situations," *Transportation Research Record: Journal of the Transportation Research Board* 2675, no. 12 (2021): 1214–1232, https://doi.org/10.1177/03611981211032650.

[25] P. Hidas, "Modelling Lane Changing and Merging in Microscopic Traffic Simulation," *Transportation Research Part C: Emerging Technologies* 10, no. 5-6 (2002): 351–371, https://doi.org/10.1016/S0968-090X(02)00026-8.

[26] A. van Beinum, H. Farah, F. Wegman, and S. Hoogendoorn, "Driving Behaviour at Motorway Ramps and Weaving Segments Based on Empirical Trajectory Data," *Transportation Research Part C: Emerging Technologies* 92 (2018): 426–441, https://doi.org/10.1016/j.trc.2018.05.018.

[27] C. M. Weyland, M. V. Baumann, H. S. Buck, and P. Vortisch, "Parameters Influencing Lane Flow Distribution on Multilane Freeways in PTV Vissim," *Procedia Computer Science* 184, no. 1 (2021): 453–460, https://doi.org/10.1016/j.procs.2021.03.057.

[28] W. Daamen, M. Loot, and S. P. Hoogendoorn, "Empirical Analysis of Merging Behavior at Freeway On-Ramp," *Transportation Research Record: Journal of the Transportation Research Board* 2188, no. 1 (2010): 108–118, https://doi.org/10.3141/2188-12.

[29] A. van Beinum, M. Hovenga, V. Knoop, H. Farah, F. Wegman, and S. Hoogendoorn, "Macroscopic Traffic Flow Changes Around Ramps," *Transportmetrica: Transportation Science* 14, no. 7 (2018): 598–614, https://doi.org/10.1080/23249935.2017.1415997.

[30] M. A. Arman and C. M. J. Tampère, "Empirical Study of Lane-Changing Maneuvers in a Weaving Area Based on Reconstructed Trajectories of Floating Car Data," *Transportation Research Record: Journal of the Transportation Research Board* 303 (2023): 30, https://doi.org/10.1177/03611981231179474.

[31] X. Chen, G. Qin, T. Seo, Y. Tian, and J. Sun, "A Macro-Micro Approach to Reconstructing Vehicle Trajectories on Multi-Lane Freeways With Lane Changing" (2023), https://doi.org/10.48550/arXiv.2306.05627.

[32] M. Treiber and D. Helbing, "Reconstructing the Spatio-Temporal Traffic Dynamics From Stationary Detector Data," *Cooperative Transportation Dynamics* 1 (2002): 3.1–3.24.

[33] L. Klitzke, K. Gimm, C. Koch, and F. Koster, "Extraction and Analysis of Highway On-Ramp Merging Scenarios From Naturalistic Trajectory Data," *2022 IEEE 25th International Conference on Intelligent Transportation Systems (ITSC)* (2022), 654–660, https://doi.org/10.1109/ITSC55140.2022.9922191.

[34] T. Toledo and D. Zohar, "Modeling Duration of Lane Changes," *Transportation Research Record: Journal of the Transportation Research Board* 1999, no. 1 (2007): 71–78, https://doi.org/10.3141/1999-08.

[35] E. Balal, R. L. Cheu, T. Gyan-Sarkodie, and J. Miramontes, "Analysis of Discretionary Lane Changing Parameters on Freeways," *International Journal of Transportation Science and Technology* 3, no. 3 (2014): 277–296, https://doi.org/10.1260/2046-0430.3.3.277.

[36] M. Treiber, A. Hennecke, and D. Helbing, "Congested Traffic States in Empirical Observations and Microscopic Simulations," *Physical Review E* 62, no. 2 (2000): 1805–1824, https://doi.org/10.1103/PhysRevE.62.1805.

[37] C. Fu and T. Sayed, "Comparison of Threshold Determination Methods for the Deceleration Rate to Avoid a Crash (DRAC)-Based Crash Estimation," *Accident Analysis and Prevention* 153 (2021): 106051, https://doi.org/10.1016/j.aap.2021.106051.

[38] M. Berghaus, S. Lamberty, J. Ehlers, E. Kalló, and M. Oeser, "Vehicle Trajectory Dataset From Drone Videos Includin ag Off-Rampnd Congested Traffic: Analysis of Data Quality, Traffic Flow, and Accident Risk," *Communications in Transportation Research* 4 (2024): 100133, https://doi.org/10.1016/j.commtr.2024.100133.

[39] T. Moers, L. Vater, R. Krajewski, J. Bock, A. Zlocki, and L. Eckstein, "The exiD Dataset: A Real-World Trajectory Dataset of Highly Interactive Highway Scenarios in Germany," in *2022 IEEE Intelligent Vehicles Symposium (IV), 2022 IEEE Intelligent Vehicles Symposium (IV)* (Aachen, Germany: IEEE, 2022), 958–964.

[40] P. A. Lopez, E. Wiessner, M. Behrisch, et al., "Microscopic Traffic Simulation Using SUMO," in *2018 21st International Conference on Intelligent Transportation Systems (ITSC), 2018 21st International Conference on Intelligent Transportation Systems (ITSC)* (Maui, HI: IEEE, 2018), 2575–2582.

[41] The MathWorks Inc, *MATLAB Version: 9.13.0 (R2022b), Natick* (Massachussetts: The MathWorks Inc. Available from, 2022), https://www.mathworks.com/.